Journal of Medicinal Chemistry

pubs.acs.org/jmc Article

2,4,5-Trisubstituted Pyrimidines as Potent HIV-1 NNRTIs: Rational Design, Synthesis, Activity Evaluation, and Crystallographic Studies

Dongwei Kang,* Francesc X. Ruiz, Yanying Sun, Da Feng, Lanlan Jing, Zhao Wang, Tao Zhang, Shenghua Gao, Lin Sun, Erik De Clercq, Christophe Pannecouque, Eddy Arnold,* Peng Zhan,* and Xinyong Liu*

Cite This: J. Med. Chem. 2021, 64, 4239−4256 Read Online

ACCESS | Metrics & More | Article Recommendations | Supporting Information

ABSTRACT: There is an urgent unmet medical need for novel human immunodeficiency virus type 1 (HIV-1) inhibitors that are effective against a variety of NNRTI-resistance mutations. We report our research efforts aimed at discovering a novel chemotype of anti-HIV-1 agents with improved potency against a variety of NNRTI-resistance mutations in this paper. Structural modifications of the lead **K-5a2** led to the identification of a potent inhibitor **16c**. **16c** yielded highly potent anti-HIV-1 activities and improved resistance profiles compared with the approved drug etravirine. The co-crystal structure revealed the key role of the water networks surrounding the NNIBP for binding and for resilience against resistance mutations, while suggesting further extension of **16c** toward the NNRTI-adjacent site as a lead development strategy. Furthermore, **16c** demonstrated favorable pharmacokinetic and safety properties, suggesting the potential of **16c** as a promising anti-HIV-1 drug candidate.

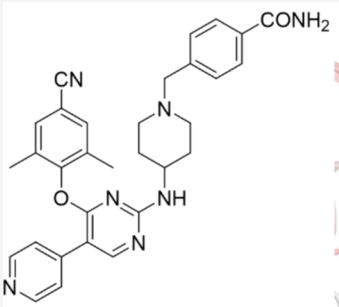

16c

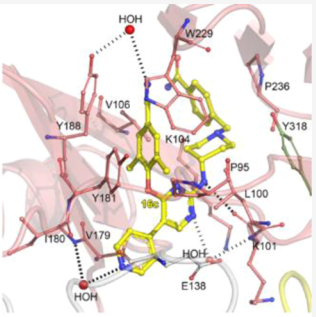

Crystal structure of 16c/RT

INTRODUCTION

Acquired immunodeficiency syndrome is caused by human immunodeficiency virus type 1 (HIV-1), becoming a pandemic health problem which globally affects nearly 38.0 million people and with 1.7 million newly infected with HIV in 2019.[1] In the HIV-1 infection process, HIV-1 reverse transcriptase (RT) is responsible for the reverse transcription of single-stranded RNA into double-stranded DNA.[2] With RT as a target, eight nucleoside/nucleotide RT inhibitors (NRTIs/NtRTIs) and six non-nucleoside RT inhibitors (NNRTIs) have been approved by the U.S. Food and Drug Administration (FDA) so far.[3,4] NRTIs are analogues of the natural substrate deoxynucleotide triphosphates, and they inhibit RT as chain terminators, while NNRTIs do not compete for the natural substrate, they bind in the NNRTI binding pocket (NNIBP) about 10 Å away from the polymerase active site known and act as allosteric inhibitors.[5] Therein, NNRTIs are widely used in combination antiretroviral therapy with the advantage of their promising antiviral activity and higher selectivity. Currently, FDA-approved NNRTIs in clinical use include the first-generation NNRTIs nevirapine (NVP), delavirdine (DLV), efavirenz (EFV) and the second generation NNRTIs etravirine (ETR), rilpivirine (RPV), and doravirine (DOR).[3,4] However, NNIBP residues are not involved in the polymerase binding site, and their mutations do not have a significant effect on replication. Thus, the NNRTIs have a low genetic barrier, and NNRTI resistance mutations appear relatively easy and fast.[5] The first-generation NNRTIs quickly suffered from drug resistance, including single mutations (K103N and Y181C) and double mutation K103N + Y181C (RES056). Although the second generation exhibited these mutations sensitive to the first-generation NNRTIs, drug resistance and cross resistance still emerged with their clinical use. In addition, the adverse effects (such as hypersensitivity reactions) can also result in treatment failure of the second-generation NNRTIs.[6,7] Therefore, there is a relevant need of novel NNRTIs with greater potency, improved drug-resistance profiles, and safety.

Our previous efforts have prompted the discovery of novel piperidine-substituted thiophene[3,2-*d*]pyrimidine compounds **3** (**K-5a2**) and **4** (**25a**) (Figure 1), exhibiting higher anti-HIV-1 potency and favorable resistance profiles compared with ETR and RPV.[8,9] The co-crystal structures revealed extensive hydrophobic interactions and a network of backbone hydrogen bonds formed between the NNRTIs and NNIBP and

Received: February 10, 2021
Published: March 18, 2021

https://doi.org/10.1021/acs.jmedchem.1c00268
J. Med. Chem. 2021, 64, 4239−4256

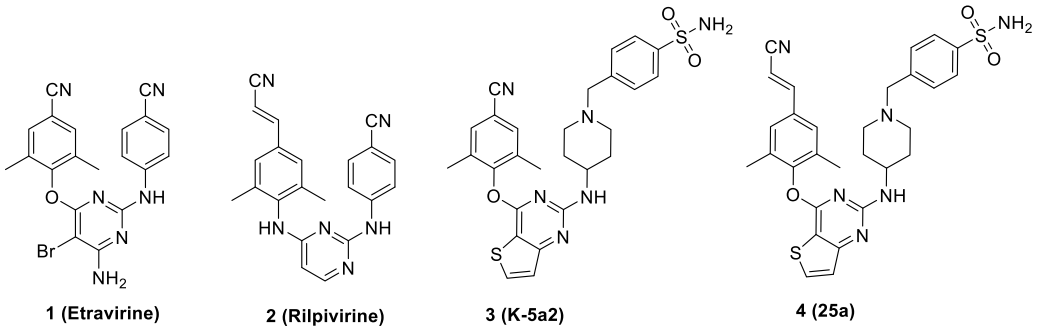

Figure 1. Chemical structures of ETR, RPV, and the piperidine-substituted thiophene[3,2-*d*]pyrimidine compounds **K-5a2** and **25a**.

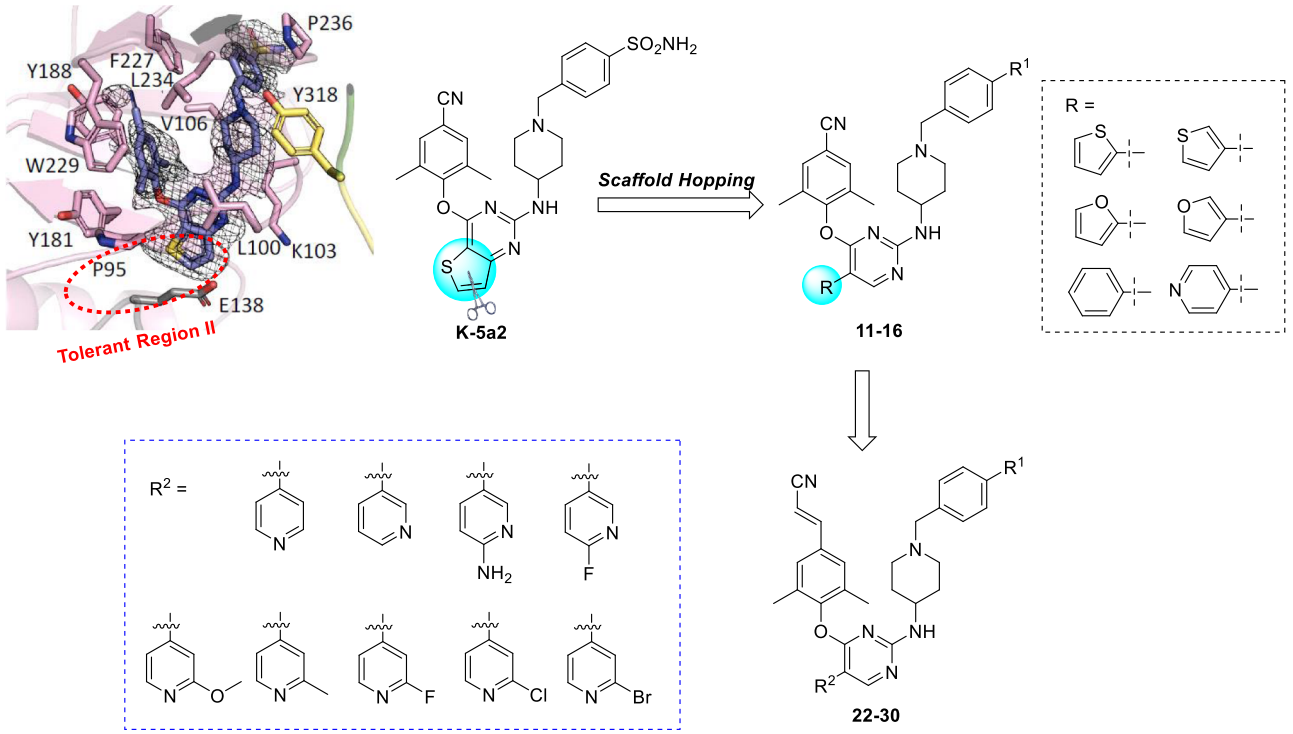

Figure 2. Rational design of novel NNRTIs bearing the 2,4,5-trisubstituted pyrimidine scaffold utilizing a scaffold hopping strategy (truncation of the fused ring).

explained why **K-5a2** and **25a** are resilient to NNRTI-resistance mutations in the NNIBP.[10] Although **K-5a2** and **25a** developed extensive interactions with NNIBP and their central thiophene[3,2-*d*]pyrimidine core establishes nonpolar interactions with the alkyl chain of Glu138, the entrance channel gated by Glu138 in the p51 subunit and Lys101 in the p66 subunit is still an underexplored region in the NNIBP.

In this study, we have kept the privileged left wing and piperidine-substituted benzyl of **K-5a2** unchanged,[8,11] and 18 novel 2,4,5-trisubstituted pyrimidine derivatives (**11**−**16**) with 2-thienyl, 3-thienyl, 2-furyl, 3-furyl, phenyl, and 4-pyridyl linked to the C_5 position of the central pyrimidines were designed utilizing a scaffold hopping strategy to get a deeper insight of the structure−activity relationships (SARs) of the NNIBP tolerant region II (Figure 2).[12] The preliminary results demonstrated that the disruption of the molecular planarity of the fused bicyclic thiophene[3,2-*d*]pyrimidine was a valuable strategy for the subsequent optimization of our lead compounds, and the introduction of a pyridine ring in the tolerant region II is the most beneficial modification for the activity. Moreover, multiple substituent groups were introduced into the pyridine ring in the second-round structural modification and yielded 27 novel derivatives. In addition, the privileged cyanovinyl group was merged into the left wing of the compounds[9,13−15] to develop stronger $\pi-\pi$ interactions with conserved amino acids F227 and W229 (Figure 2).

CHEMISTRY

As depicted in Schemes 1 and 2, two short synthetic protocols that would allow the rapid optimization of the two variable points (R^1 and Ar) were used to produce the newly designed compounds. At first, the commercially available material 2,4-dichloropyrimidine (**5**) was reacted with 4-hydroxy-3,5-dimethylbenzonitrile at room temperature (rt), affording intermediate **6**, which generated compound **7** with *tert*-butyl 4-aminopiperidine-1-carboxylate at 120 °C *via* nucleophilic reaction. Compound **7** was treated with NIS and HOAc to form compound **8**; subsequent treatment of which in the presence of trifluoroacetic acid (TFA) afforded product **9**. Then, treatment of **9** with substituted benzyl chloride (bromine) at rt yielded the key intermediates **10a**−**c**, which

https://doi.org/10.1021/acs.jmedchem.1c00268
J. Med. Chem. 2021, 64, 4239−4256

Scheme 1. Synthesis of 11−13[a]

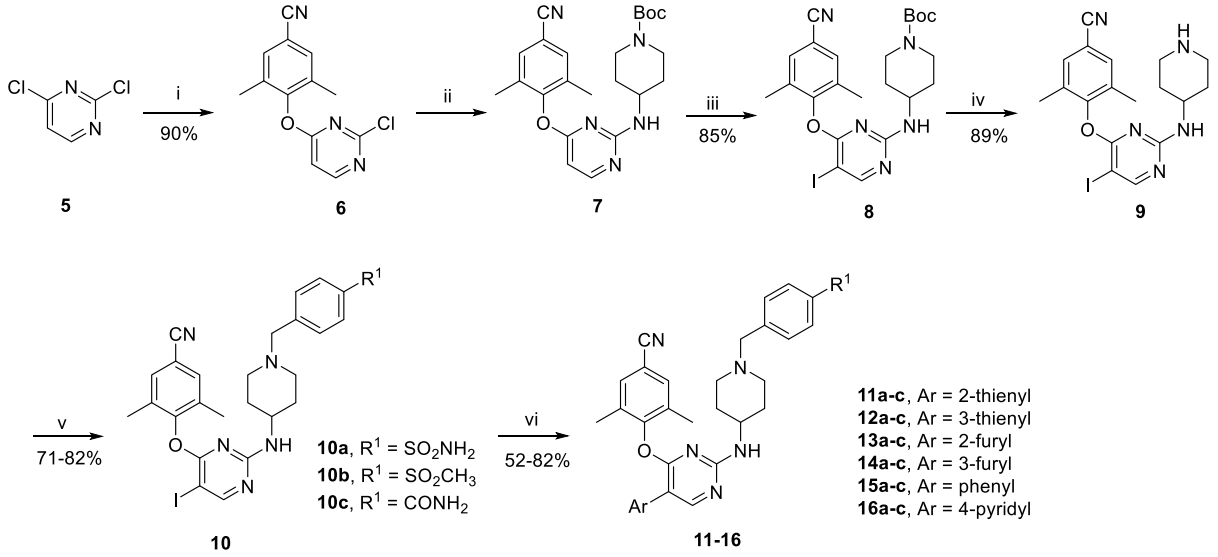

[a]Reagents and conditions: (i) K_2CO_3, dimethylformamide (DMF), 4-hydroxy-3,5-dimethylbenzonitrile, rt; (ii) K_2CO_3, DMF, *tert*-butyl 4-aminopiperidine-1-carboxylate, 120 °C; (iii) NIS, HOAc, CH_3CN, rt; (iv) TFA, dichloromethane (DCM), rt; (v) K_2CO_3, DMF, rt; (vi) $Pd(PPh_3)_4$, K_2CO_3, DMF, H_2O, 100 °C.

Scheme 2. Synthesis of 22−30[a]

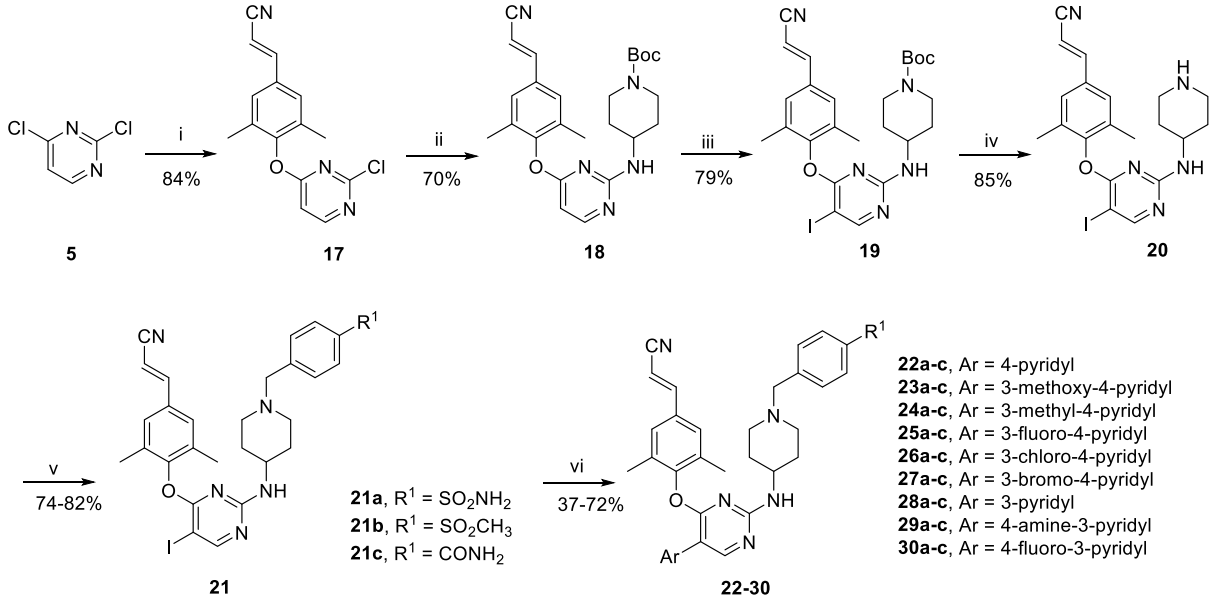

[a]Reagents and conditions: (i) (*E*)-3-(4-hydroxy-3,5-dimethylphenyl)acrylonitrile, K_2CO_3, DMF, rt; (ii) K_2CO_3, DMF, *tert*-butyl 4-aminopiperidine-1-carboxylate, 120 °C; (iii) NIS, HOAc, CH_3CN, rt; (iv) TFA, DCM, rt; (v) K_2CO_3, DMF, rt; (vi) $Pd(PPh_3)_4$, K_2CO_3, DMF, H_2O, 100 °C.

were finally coupled with boric acid substituents in the presence of potassium carbonate and $Pd(PPh_3)_4$ at 100 °C *via* Suzuki reaction, to afford the corresponding target compounds **11−16**. In an analogous way, target compounds **22−30** were prepared, only with the difference that the starting material **5** was treated with (*E*)-3-(4-hydroxy-3,5-dimethylphenyl)-acrylonitrile.

BIOLOGY

HIV-1 RT Crystallization and Structure Determination. An engineered HIV-1 RT construct, RT52A, referred to as wild-type (WT) RT, was expressed and purified as described previously.[16,17] RT52A (20 mg/mL) was incubated with **16c** at a 1:1.5 protein/drug molar ratio at rt for 30 min. Co-crystals of RT with **16c** were set up in hanging drops at 4 °C with a 1:1 ratio of the protein−ligand complex and reservoir [10% (v/v) poly(ethylene glycol) (PEG) 8000, 4% (v/v) PEG 400, 100 mM MES pH 6.3, 10 mM spermine, 15 mM $MgSO_4$, 100 mM ammonium sulfate, and 5 mM tris(2-carboxyethyl)phosphine] together with an experimentally optimized concentration of microseeds made by crushing previously obtained RT/RPV crystals (pre-seeding). The crystals were cryo-protected by dipping them into the reservoir with 25% ethylene glycol and plunge-frozen in liquid N_2. X-ray data were collected from

https://doi.org/10.1021/acs.jmedchem.1c00268
J. Med. Chem. 2021, 64, 4239−4256

three of the plunge-frozen crystals at the APS 23-ID-B beamline. The crystallographic software packages HKL2000,[18] Phenix,[19] and COOT[20] were used for data processing, structure refinement, and model building, respectively. **16c** coordinates and restraints were generated with the Grade Web Server (http://grade.globalphasing.org). The structure was solved by molecular replacement using PDB ID 4G1Q as the template. The diffraction data and refinement statistics are summarized in Table S1.

RESULTS AND DISCUSSION

First Round of Structural Modification. All of the synthesized inhibitors possessing the 2,4,5-trisubstituted pyrimidine scaffold of the first round (**11**−**16**) were first screened for their biological activity *in vitro* against WT HIV-1 (IIIB), as well as against the NNRTI-resistant strain K103N + Y181C (RES056) using the 3-(4,5-dimethylthiazol-2-yl)-2,5-diphenyltetrazolium bromide (MTT) method according to previously reported procedures,[21,22] with the aim of getting the first insight into the SAR and to identify the most promising candidates for further optimization. The second-generation NNRTI drugs ETR and RPV were selected as controls. The values of EC_{50} (anti-HIV potency), CC_{50} (cytotoxicity), and selectivity index (SI, CC_{50}/EC_{50} ratio) of the synthesized compounds were determined.

As shown in Table 1, **14a** (EC_{50} = 2.80 nM) was demonstrated to be the most promising inhibitor against HIV-1 IIIB, being comparable to the approved drug ETR (EC_{50} = 2.80 nM). Moreover, all synthesized inhibitors exhibited highly effective activity against the HIV-1 IIIB strain with EC_{50} values ranging from 2.51 to 5.93 nM. The substitution pattern of Ar and R^1 did not significantly influence the compounds' antiviral profile against HIV-1 IIIB. However, the Ar group located in the tolerant region II could result in significant differences in activity to mutant HIV-1 strain RES056. On the whole, most of the compounds experienced a dramatic activity drop to a micromolar level of inhibition against RES056. **15a**−**c** (Ar = phenyl) exhibited the weakest potency, with EC_{50} values of 427−590 nM, being much inferior to ETR (EC_{50} = 37.6 nM) and RPV (EC_{50} = 10.7 nM). Changing the phenyl substituent of **15a**−**c** to thienyl (**11a**−**c** and **12a**−**c**) and furyl (**13a**−**c** and **14a**−**c**) improved the compounds' activity (EC_{50} = 115−415 nM). More specifically, **11a**−**c** (EC_{50} = 103−134 nM) with 2-thienyl substituent exhibited more potent activity than **12a**−**c** (EC_{50} = 209−415 nM) with 3-thienyl substituent, while **13a**−**c** (EC_{50} = 218−254 nM) with 2-furyl substituent exhibited decreased activity compared to **14a**−**c** (EC_{50} = 108−172 nM) with the 3-furyl substituent. Replacement of the phenyl substituent of **15a**−**c** with 4-pyridyl substituent also increased the compounds' potency (**16a**−**c**, EC_{50} = 24.4−244 nM), especially, **16c** (EC_{50} = 24.4 nM) yielded the greatest potency against mutant strain RES056, being superior to ETR (EC_{50} = 37.6 nM) and slightly inferior to RPV (EC_{50} = 10.7 nM). Notably, **16c** displayed much lower cytotoxicity (CC_{50} = 36.0 μM) and higher SI values against HIV-1 IIIB and RES056 strain (SI = 9603 and 1474, respectively) compared to RPV (CC_{50} = 3.98 μM, SI = 3989 and 371, respectively). None of the tested compounds showed anti-HIV-2 ROD activity.

Moreover, all these compounds were further evaluated for their activity against single mutant strains L100I, K103N, Y181C, Y188L, and E138K, and double-mutant strain F227L + V106A. As displayed in Table 2, the most promising mutant HIV-1 strain RES056 inhibitor **16c** also exhibited effective potency against all tested mutant strains, with EC_{50} values of 4.26 nM (L100I), 3.79 nM (K103N), 6.79 nM (Y181C), 6.79 nM (Y188L), 10.9 nM (E138K), and 10.4 nM (F227L + V106A), being equipotent to or superior to ETR and RPV in the same cellular assay. Specifically, in the case of Y188L and F227L + V106A mutant strains, **16c** showed 11-fold and 7.8-

Table 1. Anti-HIV Activity, Cytotoxicity and SI Values of Target Compounds 11−16

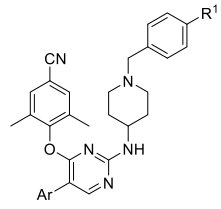

11-16

Compds	Ar	R^1	EC_{50} (nM)[a]			CC_{50}	SI[c]	
			IIIB	RES056	ROD	(μM)[b]	IIIB	RES056
11a		SO_2NH_2	4.57±0.50	103±33.8	≥33410	53.8±41.9	11787	520
11b		SO_2CH_3	4.01±0.73	134±29.8	>8383	8.38±4.50	2091	62
11c		$CONH_2$	3.34±1.17	115±6.71	>9263	9.26±3.75	2773	80
12a		SO_2NH_2	5.09±1.50	209±40.7	>6124	6.13±1.98	1205	29
12b		SO_2CH_3	4.92±1.60	253±83.8	>4252	4.25±1.45	863	17
12c		$CONH_2$	4.22±0.38	415±76.4	>37332	37.3±4.31	8838	90
13a		SO_2NH_2	4.40±1.26	218±100	>11187	11.2±2.92	2539	51
13b		SO_2CH_3	4.52±1.03	233±45.6	>7459	7.45±3.27	1650	32
13c		$CONH_2$	5.78±1.45	254±66.4	>7347	7.35±2.46	1271	29
14a		SO_2NH_2	2.51±0.73	161±40.9	>29105	29.1±8.99	11611	180
14b		SO_2CH_3	4.75±0.94	172±9.51	>55821	55.8±13.7	11748	323
14c		$CONH_2$	3.40±0.48	108±24.5	>181990	181±7.10	53580	1685
15a		SO_2NH_2	5.14±2.08	427±62.6	>14067	14.1±4.72	2735	33
15b		SO_2CH_3	4.93±1.75	590±103	>12118	12.1±5.26	2456	21
15c		$CONH_2$	5.11±2.13	562±75.9	>13367	≥13.37	≥2618	≥24
16a		SO_2NH_2	2.59±0.46	111±35.9	>5669	5.67±0.27	2189	51
16b		SO_2CH_3	5.93±2.79	244±45.8	>17197	17.2±4.09	2897	70
16c		$CONH_2$	3.75±0.40	24.4±3.06	>35998	36.0±4.85	9603	1474
ETR	-	-	2.80±0.65	37.6±2.09	>4594	>4.59	>1638	>122
RPV			1.00±0.27	10.7±7.96	-	3.98	3989	371

[a]EC_{50}: concentration of compound required to achieve 50% protection of MT-4 cell cultures against HIV-1-induced cytopathicity, as determined by the MTT method. [b]CC_{50}: concentration required to reduce the viability of mock-infected cell cultures by 50%, as determined by the MTT method. [c]SI: selectivity index, the ratio of CC_{50}/EC_{50}.

https://doi.org/10.1021/acs.jmedchem.1c00268
J. Med. Chem. 2021, 64, 4239−4256

Table 2. Activity against Mutant HIV-1 Strains of Target Compounds 11−16

	EC_{50} (nM)[a]					
compounds	L100I	K103N	Y181C	Y188L	E138K	F227L + V106A
11a	5.92 ± 1.11	5.39 ± 1.58	10.7 ± 3.63	9.31 ± 1.28	7.71 ± 1.86	30.2 ± 2.43
11b	8.93 ± 3.62	5.71 ± 1.46	11.6 ± 5.99	15.4 ± 4.30	6.27 ± 0.35	38.4 ± 9.65
11c	14.7 ± 2.59	5.15 ± 0.90	10.2 ± 4.68	17.9 ± 5.48	8.85 ± 1.90	75.4 ± 21.9
12a	15.4 ± 5.52	4.70 ± 0.97	12.3 ± 2.21	30.3 ± 5.84	19.7 ± 6.52	85.3 ± 15.6
12b	20.3 ± 5.08	4.75 ± 1.16	11.7 ± 2.04	27.2 ± 9.63	10.6 ± 2.80	67.5 ± 21.4
12c	62.6 ± 12.1	5.52 ± 0.85	26.4 ± 6.79	30.0 ± 12.49	22.0 ± 7.28	325 ± 95.5
13a	20.9 ± 10.5	5.33 ± 1.42	24.8 ± 11.8	36.5 ± 14.3	24.5 ± 5.57	128 ± 46.6
13b	20.4 ± 4.24	5.92 ± 0.90	26.4 ± 10.0	28. 8 ± 10.6	27.4 ± 7.81	110 ± 32.1
13c	38.2 ± 11.3	3.73 ± 0.48	14.9 ± 3.89	23.3 ± 2.89	11.9 ± 2.12	161 ± 26.7
14a	13.6 ± 7.53	3.00 ± 0.27	9.35 ± 3.88	15.3 ± 5.08	13.0 ± 1.13	63.2 ± 11.5
14b	14.8 ± 3.99	4.39 ± 0.66	14.4 ± 4.40	24.2 ± 3.50	15.3 ± 4.23	41.5 ± 6.88
14c	10.1 ± 1.75	3.44 ± 0.16	9.81 ± 1.49	21.1 ± 3.27	11.2 ± 4.12	307 ± 7.28
15a	53.2 ± 6.18	7.74 ± 0.82	26.2 ± 7.23	33.2 ± 2.51	24.5 ± 2.10	219 ± 62.4
15b	71.7 ± 12.4	11.7 ± 2.25	33.7 ± 12.1	35.5 ± 1.47	32.1 ± 4.55	218 ± 47.6
15c	151 ± 84.2	9.15 ± 2.14	28.7 ± 6.81	30.5 ± 8.73	17.1 ± 5.43	393 ± 28.4
16a	10.6 ± 2.13	2.33 ± 0.61	6.93 ± 1.36	21.4 ± 3.82	8.12 ± 0.17	45.9 ± 2.43
16b	17.4 ± 9.08	4.40 ± 0.96	10.8 ± 2.43	18.5 ± 3.37	9.19 ± 0.79	79.4 ± 13.9
16c	4.26 ± 0.62	3.79 ± 0.42	6.79 ± 1.49	6.79 ± 2.82	10.9 ± 5.63	10.4 ± 5.30
ETR	5.42 ± 1.80	2.71 ± 0.96	13.6 ± 3.56	13.7 ± 4.85	7.17 ± 2.78	17.5 ± 5.14
RPV	1.54 ± 0.00	1.31 ± 0.36	4.73 ± 0.48	79.4 ± 0.77	5.75 ± 0.11	81.6 ± 21.2

[a]EC_{50}: concentration of compound required to achieve 50% protection of MT-4 cell cultures against HIV-1-induced cytopathicity, as determined by the MTT method.

fold activity enhancement over RPV (EC_{50} = 79.4 and 81.6 nM), respectively.

In addition, most compounds were potent inhibitors against K103N, Y181C, Y188L, and E138K strains, with EC_{50} values ranging from 2.33 to 35.5 nM. However, apart from **16c**, all the compounds exhibited inferior potency (EC_{50} = 5.92−151 and 30.2−393 nM, respectively) compared to ETR (EC_{50} = 5.42 and 17.5 nM, respectively) against the L100I and F227L + V106A strains. The first round of SAR results indicated that among all the employed substituents in the first round of this study, the 4-pyridyl group was the best choice for the NNIBP tolerant region II.

Second Round of Structural Modification. Based on the preliminarily established SARs, 27 novel 2,4,5-trisubstituted pyrimidine derivatives (**22**−**30**) were designed with the most promising inhibitor **16c** as the lead. These newly designed compounds retained the privileged piperidine-substituted benzyl as their right wing; the cyano group in the left wing was replaced with a cyanovinyl group to develop stronger $\pi-\pi$ interactions with the highly conserved residues F227 and W229;[9] meanwhile, fluorine, chlorine, bromine, methyl, methoxy, and amino substituents were also introduced into the 4-pyridyl moiety located in tolerant region II to explore the SARs of tolerant region II more comprehensively. All derivatives **22**−**30** from the second round were assayed *in vitro* for their activity against HIV-1 IIIB and RES056. The results of this evaluation are summarized in Tables 3a and 3b.

The compounds generated in the second round contain the privileged 2,4,5-trisubstituted pyrimidine scaffold and displayed nanomolar activity against HIV-1 IIIB with EC_{50} values of 3.95−8.26 nM, being comparable to those of ETR (EC_{50} = 3.53 nM). More encouragingly, their activity against the mutant HIV-1 strain RES056 was significantly increased, yielding EC_{50} values ranging from 20.4 to 40.3 nM and being about 2-fold more potent than ETR (EC_{50} = 52.2 nM), with the exception of compounds **25c** (EC_{50} = 53.4 nM) and **26c** (EC_{50} = 81.7 nM). However, the introduction of a cyanovinyl group substituent resulted in these compounds having enhanced cytotoxicity (CC_{50} = 2.10−25.3 μM) compared to the lead **16c** (CC_{50} = 36.0 μM). Although the cyanovinyl group was favorable for improving potency against mutant strains, it could result in potential covalent binding with nucleic acids or proteins as a "Michael acceptor" and cause an increase of cytotoxicity.[21] When comparing the cytotoxicity of these target compounds, **28a**−**c** tolerating the 3-pyridyl in the tolerant region II showed the lowest cytotoxicity, exhibiting CC_{50} values of 20.4−25.3 μM. However, harboring an amino group or fluorine atom on the 3-pyridyl substituent resulted in compounds **29a**−**c** (CC_{50} = 2.39−12.8 μM) and **30a**−**c** (CC_{50} = 6.05−20.9 μM), respectively, which resulted in increased cytotoxicity. Replacing the 3-pyridyl of **28a**−**c** with 4-pyridyl resulted in compounds **22a**−**c** (CC_{50} = 7.20−10.2 μM), which exhibited enhanced cytotoxicity. Also, the introduction of fluorine, chlorine, bromine, methyl, methoxy, or amino substituent on the 4-pyridyl moiety of **22a**−**c** led to greater cytotoxicity.

Furthermore, eight compounds (**22a**, **22c**, **28a**−**c**, **29c**, **30a**, and **30c**) that exhibited higher potency and lower cytotoxicity were further evaluated for their activity against HIV-1 viral isolates carrying a variety of NNRTI-resistance mutations. As depicted in Table 4, although most of the selected compounds demonstrated more potent activity against L100I, Y181C, E138K, and F227L + V106A strains than did ETR, all of the compounds exhibited inferior potency (EC_{50} = 3.84−7.50, and 22.7−54.2 nM, respectively) compared to ETR (EC_{50} = 3.77 and 1.31 nM, respectively) and RPV (EC_{50} = 18.8 and 5.75 nM, respectively) for the most common mutant strains K103N and Y188L. The anti-HIV-1 results of two rounds of structural modification led to the conclusion that compound **16c** was the most potent among all the novel synthesized compounds, exhibiting higher potency against a panel of NNRTI-resistant strains than ETR and deserving further druggability evaluation.

https://doi.org/10.1021/acs.jmedchem.1c00268
J. Med. Chem. 2021, 64, 4239−4256

Table 3a. Anti-HIV Activity, Cytotoxicity, and SI Values of Target Compounds 22−28

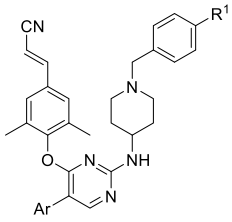

Compds	R1	R2	EC50 (nM)[a]		CC50	SI[c]	
			IIIB	RES056	(μM)[b]	IIIB	RES056
22a		SO_2NH_2	4.60±1.14	22.9±7.07	9.25±5.17	2011	404
22b		SO_2CH_3	5.74±1.38	26.3±6.99	7.20±5.41	1255	273
22c		$CONH_2$	4.19±0.45	23.3±7.67	10.2±6.69	2428	436
23a		SO_2NH_2	5.75±1.27	34.3±13.2	5.50±1.98	957	160
23b		SO_2CH_3	3.95±0.54	30.0±12.4	2.10±0.95	533	70
23c		$CONH_2$	7.28±1.27	40.3±10.7	6.27±1.21	861	156
24a		SO_2NH_2	4.16±0.98	23.0±5.85	4.37±1.15	1105	190
24b		SO_2CH_3	4.55±0.61	31.5±5.50	5.34±2.87	1174	169
24c		$CONH_2$	3.53±0.38	18.1±0.30	6.51±2.82	1845	358
25a		SO_2NH_2	6.37±1.27	38.8±12.6	8.46±2.08	1326	218
25b		SO_2CH_3	4.75±1.19	25.1±7.23	5.03±1.72	1057	200
25c		$CONH_2$	8.26±1.79	53.4±30.9	15.5±5.32	1878	290
26a		SO_2NH_2	4.30±0.54	20.9±4.14	3.89±1.01	904	185
26b		SO_2CH_3	4.23±1.06	33.3±7.24	2.04±0.88	482	61
26c		$CONH_2$	4.14±0.43	81.7±61.7	19.1±1.66	4627	243
27a		SO_2NH_2	4.42±0.52	26.9±12.1	6.60±2.69	1493	246
27b		SO_2CH_3	4.52±0.55	33.2±9.31	3.21±0.61	711	97
27c		$CONH_2$	7.00±4.69	32.2±8.02	9.45±4.34	1351	293
28a		SO_2NH_2	5.04±2.07	25.8±9.45	20.4±4.11	4063	793
28b		SO_2CH_3	4.57±1.24	22.4±1.87	23.5±0.96	5151	1049
28c		$CONH_2$	4.78±2.57	23.1±3.80	25.3±1.84	5297	1092

[a]EC_{50}: concentration of compound required to achieve 50% protection of MT-4 cell cultures against HIV-1-induced cytopathicity, as determined by the MTT method. [b]CC_{50}: concentration required to reduce the viability of mock-infected cell cultures by 50%, as determined by the MTT method. [c]SI: selectivity index, the ratio of CC_{50}/EC_{50}.

Inhibition of WT HIV-1 RT by the Representative Compounds. Some representative compounds (**14a**, **16c**, **22a**, and **22c**) were assayed *in vitro* for their ability to inhibit recombinant WT HIV-1 RT enzyme, and the results are summarized in Table 5. **14a**, **16c**, **22a**, and **22c** (IC_{50} = 0.092, 0.113, 0.143, and 0.102 μM, respectively) exhibited modest inhibitory activity against WT HIV-1 RT with IC_{50} values of 0.092, 0.113, 0.143, and 0.102 μM, being about 3.5−5.5-fold potent than NVP (IC_{50} = 0.510 μM). Although these novel inhibitors exhibited inferior activity compared to ETR (IC_{50} = 0.012 μM), the preliminary results validate their binding target as HIV-1 RT, and they are classical NNRTIs.

Crystal Structure of HIV-1 RT in Complex with 16c: Implications for Further Lead Development. To observe the detailed interactions between **16c** and the NNIBP (formed by three channels named tunnel, entrance, and groove), the co-crystal structure of WT RT in complex with **16c** was determined at 2.02 Å resolution (Table S1 and Figure S1). As expected, the structure was almost identical to that of the related RT complexes with **K-5a2** and **25a** (Figure S1F). Figure 3A depicts the main interactions of **16c** with RT. The left wing of **16c** is snuggling into the tunnel *via* hydrophobic interactions with Y181 and Y188 at one side and P95 and L234 at the other. Meanwhile, the right wing is anchored into the groove by a hydrogen bond with the main-chain carbonyl of K101 and through hydrophobic contacts with L100, Y318, and P236. The central pyrimidine moiety is located in the entrance, surrounded by E138 of p51, L100 (hydrophobic contacts), and K101 (hydrogen-bonded to the main-chain amino group through a water bridge).

The 4-pyridyl substituent, as envisioned, sits in the solvent-exposed area in the vicinity of the entrance channel, displacing three water molecules (modeled in the RT/**16c** structure as an alternate conformation) observed in the RT/RPV high resolution structure (Figures 3B and S1B,E).[23] Moreover, it forms hydrophobic interactions with the side chains of V179 and Y181, and it is water-bridged to the main-chain carbonyl of I180 (Figure 3B). Notably, in all three RT structures with **K-5a2**, **25a**, and RPV, their central ring forms a water-mediated hydrogen bonding network with the main-chain atoms of E138 and of I180.[10,23] Herein, the water molecule hydrogen-bonded to the central ring and E138 is displaced (alt-HOH 1 in Figure 3B), but the second water molecule hydrogen-bonded to I180 is conserved.

The RT/**16c** structure illustrates the importance of ordered water networks in NNRTI binding (Figure 3C−E). The left wing of **16c** makes a hydrogen bond with an interfacial water that is in turn hydrogen-bonded to the side chain of Y188 and the main chain of L228 (Figure 3C). Next, as mentioned, the entrance channel displays another interfacial water, which is connected to a succession of water molecules that end up in a water molecule bridging Q161, T165, and Q182, the latter being hydrogen-bonded to the main chain of M184 (Figure 3D), a residue that is part of the catalytic motif YMDD.[24] Both the left wing interfacial water and the ordered network near the entrance channel are observed in the RT/RPV high resolution structure (data not shown).[23] Lastly, the right wing of **16c** is also interacting with a water network bridging it to RT (Figure 3E). Central to it, HOH 2 connects the pyrimidine ring with the main chain of K101. At one end, the water network ends with HOH 1, hydrogen-bonded to p51's E138 side chain. At the other end, the water network finishes with HOH 4, which would be in the right position to be bonded to alt-HOH 3, expelled by the binding. The last is hydrogen bonded to the other carboxylic oxygen of p51's E138 side chain. This network is observed, albeit with some discontinuity, in the case of parent lead **K-5a2**. Interestingly, in the RT/RPV structure, there is a direct hydrogen bond between the main chain of K101 and the central ring, while the terminal amino group of the side chain of K101 overlaps with HOH 1 of RT/**16c** (present also in RT/**K-5a2**). Thus, in a different manner, all

https://doi.org/10.1021/acs.jmedchem.1c00268
J. Med. Chem. 2021, 64, 4239−4256

Table 3b. Anti-HIV Activity, Cytotoxicity, and SI Values of Target Compounds 29−30

Compds	R^1	R^2	EC_{50} (nM)[a]		CC_{50}	SI[c]	
			IIIB	RES056	(μM)[b]	IIIB	RES056
29a	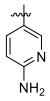	SO_2NH_2	5.80±1.37	33.5±6.89	2.91±0.65	503	87
29b	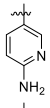	SO_2CH_3	5.29±2.14	26.2±4.80	2.36±0.93	447	90
29c	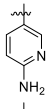	$CONH_2$	6.56±2.11	30.2±6.55	12.8±3.73	1956	424
30a	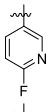	SO_2NH_2	5.80±1.53	28.2±6.82	17.1±4.82	2956	607
30b	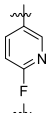	SO_2CH_3	6.04±1.76	25.5±2.89	6.05±1.18	1003	237
30c	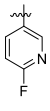	$CONH_2$	4.56±1.49	20.4±0.98	20.9±3.65	4586	1021
ETR	-	-	3.53±0.70	52.2±24.2	>4.59	>1300	>88
RPV			1.0±0.27	10.7±7.96	3.98	3989	371

[a]EC_{50}: concentration of compound required to achieve 50% protection of MT-4 cell cultures against HIV-1-induced cytopathicity, as determined by the MTT method. [b]CC_{50}: concentration required to reduce the viability of mock-infected cell cultures by 50%, as determined by the MTT method. [c]SI: selectivity index, the ratio of CC_{50}/EC_{50}.

Table 4. Activity against Mutant HIV-1 Strains

	EC_{50} (nM)[a]					
compounds	L100I	K103N	Y181C	Y188L	E138K	F227L + V106A
22a	5.87 ± 1.99	4.91 ± 1.47	24.2 ± 8.96	27.1 ± 9.19	11.1 ± 2.21	23.7 ± 13.8
22c	5.62 ± 1.98	3.84 ± 0.66	7.14 ± 1.07	23.0 ± 4.49	8.66 ± 0.37	35.5 ± 21.6
28a	7.85 ± 3.59	6.25 ± 4.17	9.95 ± 0.96	25.1 ± 12.7	11.9 ± 2.35	12.2 ± 2.27
28b	10.7 ± 1.54	5.42 ± 2.35	10.3 ± 1.32	22.7 ± 9.14	12.2 ± 4.53	13.2 ± 3.41
28c	10.8 ± 1.66	5.76 ± 2.33	10.1 ± 1.62	25.5 ± 12.3	11.3 ± 2.74	21.7 ± 9.43
29c	11.3 ± 3.73	6.66 ± 0.50	12.0 ± 1.45	54.2 ± 10.9	15.4 ± 3.98	15.4 ± 3.22
30a	11.4 ± 2.85	7.50 ± 1.61	15.4 ± 2.24	36.7 ± 6.86	49.1 ± 31.5	23.1 ± 13.9
30c	5.76 ± 3.50	5.97 ± 1.49	10.3 ± 0.53	30.1 ± 10.9	11.7 ± 6.16	27.5 ± 10.5
ETR	11.7 ± 7.44	3.77 ± 1.06	16.6 ± 5.36	15.4 ± 4.72	18.8 ± 8.52	26.9 ± 2.30
RPV	1.54 ± 0.00	1.31 ± 0.36	4.73 ± 0.48	79.4 ± 0.77	5.75 ± 0.11	81.6 ± 21.2

[a]EC_{50}: concentration of compound required to achieve 50% protection of MT-4 cell cultures against HIV-1-induced cytopathicity, as determined by the MTT method.

Table 5. Inhibitory Activity against WT HIV-1 RT

compounds	IC_{50} (μM)[a]	compounds	IC_{50} (μM)[a]
14a	0.092 ± 0.002	**22a**	0.143 ± 0.003
16c	0.113 ± 0.032	**22c**	0.102 ± 0.013
NVP	0.510 ± 0.140	ETR[b]	0.011 ± 0.000

[a]IC_{50}: inhibitory concentration required to inhibit biotin deoxyuridine triphosphate incorporation into WT HIV-1 RT by 50%. [b]Results from ref 11.

three complexes maintain a similar architecture in that part in between the entrance and the groove channels.

The RT/**16c** structure suggests that not only the hydrogen bonds in the right wing and the several hydrophobic contacts all around the ligand but also the water molecules (and networks) may anchor the compound in the NNIBP. While in the current structure the right-wing top amide group is not hydrogen-bonded (or with a polar interaction) with RT or has water molecules in the vicinity, both RPV (*i.e.*, nitrile substituent of the right wing with the carbonyl group of H235) and **K-5a2** (*i.e.*, hydrogen bonds to K104 and V106) present one or the other. In the case of RT/RPV, molecular dynamics (MD) simulations suggest as well the existence of a

https://doi.org/10.1021/acs.jmedchem.1c00268
J. Med. Chem. 2021, 64, 4239−4256

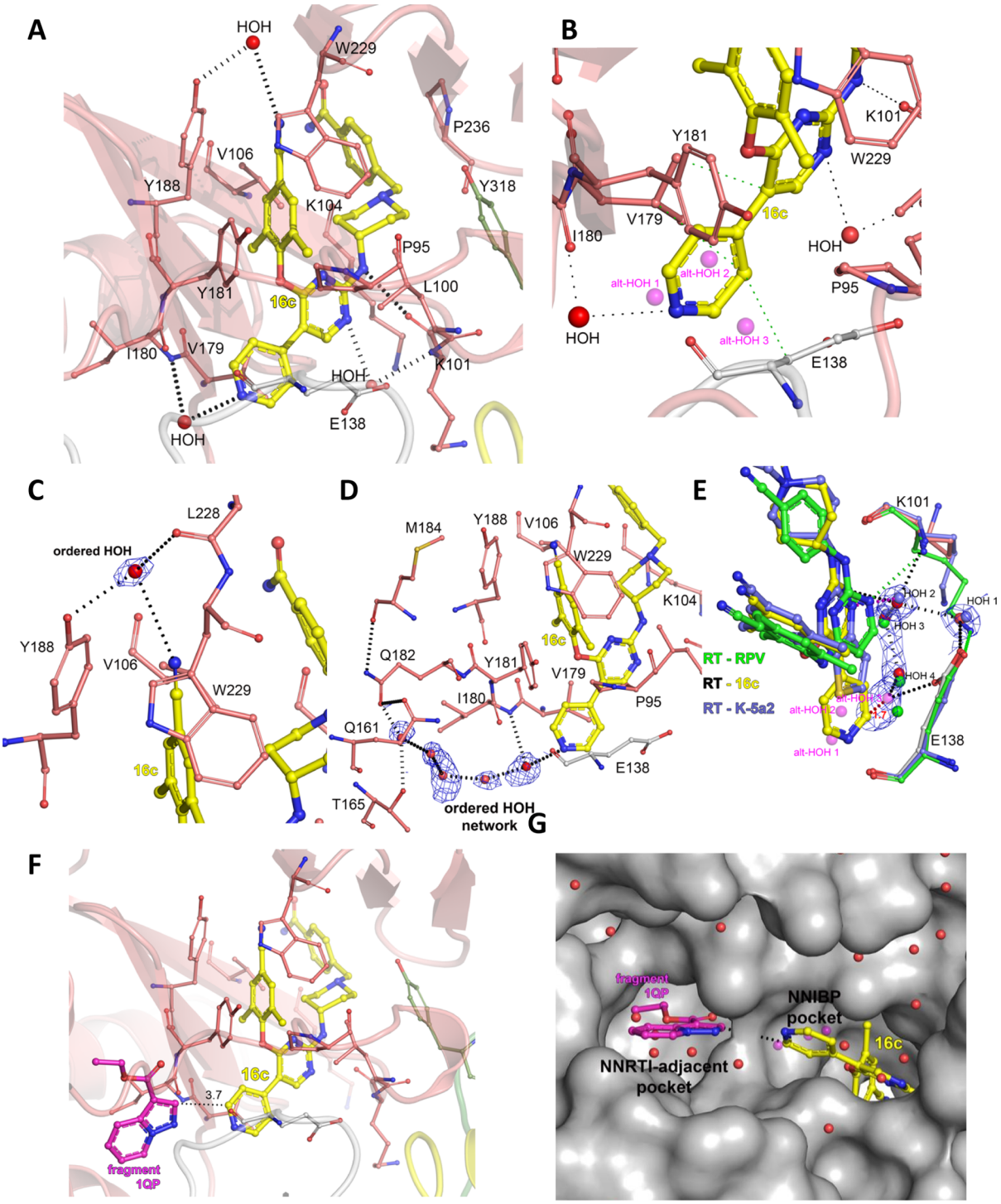

Figure 3. Crystal structure of HIV-1 RT in complex with **16c** (PDB ID: 7KWU). (A) **16c** binding in the NNIBP, with hydrogen bonding interactions with RT and water molecules. (B) Detail of the binding of the 4-pyridyl substituent. (C−E) Water molecule and networks involved in binding of **16c**. (F) Overlay of the RT/**16c** structure with RT/RPV-1QP fragment (bound to the NNRTI adjacent site, PDB ID 4KFB), with the distance between nearer atoms of each. (G) Surface representation of (F), displaying the labeled pockets, with surrounding crystallographic water molecules from the RT/**16c** structure. Color legend for carbon atoms: (i) RT p66 subdomains: fingers in blue, palm in dark red, thumb in green, and connection in yellow; (ii) RT p51 subunit in white, and water molecules in red unless otherwise indicated.

water molecule hydrogen-bonded to the benzonitrile in the right wing, as this area is solvent exposed.[10,23]

Regarding the SAR, the structure points to all the different compounds binding roughly identically in terms of both the two wings and the central core, as well as for the different Ar substituents. Indeed, this is supported by the very similar antiviral activity of all of the tested compounds against strain IIIB (Tables 1−4) and in the *in vitro* activity assay (Table 5). The Ar substituents may thus displace the alternative conformation water molecules and will be engaged in hydrophobic contacts with the side chains of V179 and Y181 (Figure 3B). Meanwhile, the water-bridged interaction with

https://doi.org/10.1021/acs.jmedchem.1c00268
J. Med. Chem. 2021, 64, 4239−4256

Table 6. Pharmacokinetic Profile of 16c[a]

subject	$T_{1/2}$ (h)	T_{max} (h)	C_{max} (ng/mL)	AUC_{0-t} (h ng/mL)	$AUC_{0-\infty}$ (h ng/mL)	CL (mL/min/kg)	F (%)
16c (iv)[b]	2.46 ± 0.56	0.033	278 ± 31.2	293 ± 32.7	303 ± 31.1	110 ± 10.9	
16c (po)[c]	1.74 ± 0.65	1.00 ± 0.00	174 ± 12.5	460 ± 296	466 ± 294		15.3

[a]PK parameter (mean ± standard deviation, n = 3). [b]Dosed intravenously at 2 mg/kg. [c]Dosed orally at 20 mg/kg.

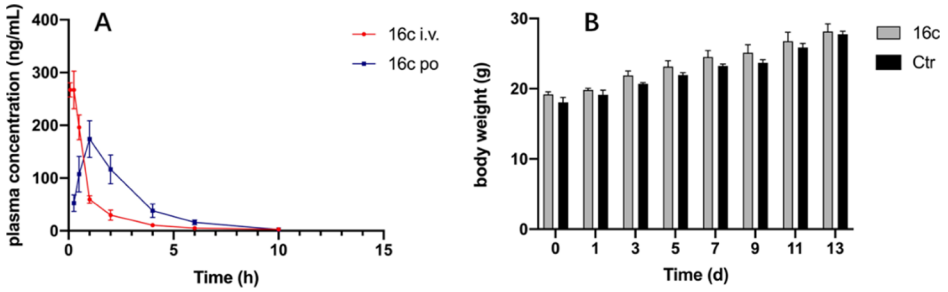

Figure 4. (A) Plasma concentration−time profiles of **16c** in rats following oral administration (20 mg/kg) and iv administration (2 mg/kg). (B) Relative body weight changes of Kunming mice in different groups.

I180 is potentially possible in all the compounds bearing an electronegative atom in the ring, able to function as a hydrogen bond acceptor. However, the geometry and/or distance may not be ideal in the five-membered rings. This interaction may be critical in the case of mutant strain RES056, where just compound **16c** can retain a similar antiviral activity as in the WT IIIB strain.

Structures of the K103N/Y181C mutant RT with RPV and compound **3** (**25a**) show that either the repositioning of the aromatic side chain of Y183 and/or maintaining the hydrogen-bonding interactions in the right wing may provide these adaptable compounds a similar tight interaction with WT RT.[10] Nevertheless, these interactions are expected to occur as well for both **16c** and the rest of compounds. Therefore, the interfacial water-mediated contact with I180 (connected to an extensive water network) may be the difference. This contact is not possible in compounds **15a−c** and likely suboptimal or not existing for compounds of the **11−14** series. What happens then with compounds **16a** and **16b**? The response is not apparent from this series but from the second round of compounds designed after **16c** (Tables 3a and 3b). Compounds **22−30**, also resilient to K103N/Y181C mutations as **16c**, differ from compounds of the **16** series in that the ring wing bears the cyanovinyl group substituent instead of the cyano.

Notably, our previous high-resolution RT/RPV structure, combined with infrared spectroscopy experiments and MD simulations of WT and K103N/Y181C mutant RT,[23] shows that the conserved interaction of the cyanovinyl group with a water molecule contributes to the enhanced binding of RPV in both the WT and the mutant. This water molecule is conserved in the RT/**16c** structure, the first time this is observed with a left wing benzonitrile substituent. Thus, while the geometry is similar, the hydrogen bond is weaker in the current structure (2.7 Å in RT/RPV *vs* 3.7 Å in RT/**16c**). We surmise that **16c**, but not **16a** or **16b**, is the only compound of the first round series presenting this water molecule (which in the RT/RPV structure is seen connected to a water network extending toward residues 224−226). Accordingly, compounds **22−30**, with the longer cyanovinyl group likely forming this water interaction, cope similarly well with the K103N/Y181C mutations irrespective of the R^1 substituent.

Overall, the analysis of the RT/**16c** structure and related SAR put the spotlight on the key role of the water networks around the NNIBP for tight ligand binding to both WT and mutant RT. In relation to it, several recent papers, by combining MD simulations, high resolution X-ray and neutron crystallography, and isothermal titration calorimetry, have shown the paramount role of this kind of water networks in ligand binding, suggesting that "solvent structure is an evolutionary constraint on protein sequence that contributes to ligand affinity and selectivity."[25−27]

We also have recognized that the 4-pyridyl substituent extends out of the NNIBP in the direction of fragment 1QP (Figure 3F,G) sitting on the NNRTI-adjacent site,[16] which may allow fragment linking/merging approaches. It should be noted that fragment 1QP displaces most of the water molecules forming the water network shown in Figure 3D. Taking into account that the 4-pyridyl substituent displaces the water molecules near the entrance channel, a compound targeting both pockets, as designed and tested by us recently, will displace all the water molecules out of these pockets and likely accounting for an entropic gain.[28] Therefore, the further development of these kind of compounds is warranted. The second round of optimization also encourages us to further pursue this direction, as the substitutions assayed were probably oriented toward the solvent area (because of the likely penalty of facing the protein side, *i.e.*, near residue I180 main chain), not resulting in any improvement in comparison to **16c**.

***In Vivo* Pharmacokinetics Study.** The *in vivo* pharmacokinetic profile of **16c** was evaluated in Sprague Dawley rats (Table 6 and Figure 4A). After a single 2 mg/kg intravenous (iv) dose, compound **16c** was characterized by a modest clearance (CL = 110 mL/min/kg) and half-life ($T_{1/2}$ = 2.46 h), the maximum concentration (C_{max}) could be up to 278 ng/mL. Absorption of **16c** was evaluated after being dosed at 20 mg/kg, it reached maximum concentration (T_{max}) at 1.00 h with a C_{max} of 174 ng/mL and the half-life was 1.74 h. However, the oral bioavailability (F) was 15.3%, which need further improvement for a drug candidate.

Safety Assessment. *Assessment of Acute Toxicity.* Next, the acute toxicity test of **16c** was carried out. A total of 20 Kunming mice were randomly divided into two groups and

https://doi.org/10.1021/acs.jmedchem.1c00268
J. Med. Chem. 2021, 64, 4239−4256

given single oral doses of 0 mg/kg (control group) and 2000 mg/kg of **16c** on the first day, respectively. The mice did not exhibit any toxic symptoms or mortality immediately during the subsequent two weeks. Additionally, there was no abnormality of body weight changed (Figure 4B). The results demonstrated that **16c** was well-tolerated up to a dose of 2000 mg/kg with no acute toxicity.

Assessment of hERG Activity. With the aim to estimate the potential risk for cardiotoxicity, **16c** was evaluated for its activity against the human ether-à-go-go related gene (hERG) potassium channel using manual patch-clamp electrophysiology approach, and terfenadine was selected as a reference drug. As shown in Figure 5, **16c** exhibited an IC_{50} value of 1.19 μM

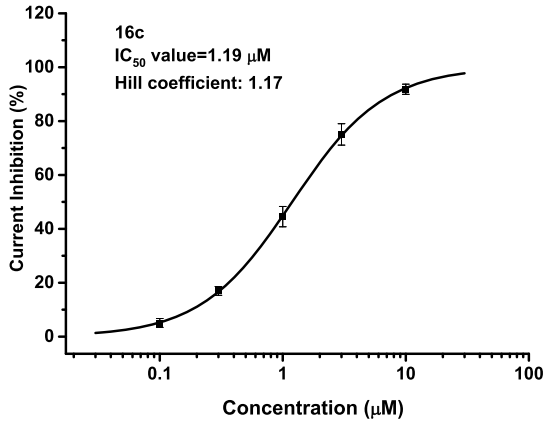

Figure 5. Activity of **16c** against hERG potassium channel in HEK293 cells.

and demonstrated much reduced QT liability and lower hERG inhibition in comparison with the lead **K-5a2** (IC_{50} = 0.130 μM) and the approved NNRTIs drug RPV (IC_{50} = 0.50 μM).[29]

CONCLUSIONS

We have reported herein efforts to discover novel potent HIV-1 inhibitors by exploiting the underexplored tolerant region II of the NNIBP, and forty-five novel 2,4,5-trisubstituted pyrimidine derivatives were designed using a scaffold hopping approach. Notably, we could demonstrate that compound **16c**, designed by introducing a 4-pyridyl group in the C_5 position of the central pyrimidine scaffold, led to improved anti-HIV-1 potency against WT and mutant HIV-1 strains compared to ETR, with EC_{50} values of 3.75 nM (WT), 4.26 nM (L100I), 3.79 nM (K103N), 6.79 nM (Y181C), 6.79 nM (Y188L), 10.9 nM (E138K), 10.4 nM (F227L + V106A), and 24.4 nM (RES056) in MT-4 cells. Moreover, **16c** exhibited lower cytotoxicity (CC_{50} = 36.0 μM), which contribute to its higher SI values toward WT and mutant HIV-1 strains. Additionally, **16c** exhibited *in vivo* favorable pharmacokinetic properties in Sprague Dawley rats (F = 15.3%) and safety in Kunming mice (LD_{50} > 2000 mg/kg).

The co-crystal structure and the SAR analysis, on the basis of the previous crystallographic and spectroscopic experiments and MD simulations, revealed that the water networks surrounding the NNIBP, both on top and on the bottom, may work as a sort of molecular staples anchoring the NNRTIs and allowing them to "wiggle and jiggle" (*i.e.*, conformational and positional adaptability) when resistance mutations arise. Furthermore, they provide a framework for an improved structure-based drug design of NNRTIs, especially those targeting simultaneously the NNIBP and the NNRTI adjacent site.

EXPERIMENTAL SECTION

Chemistry. All melting points were determined on a micro melting point apparatus and are uncorrected. ^{1}H NMR and ^{13}C NMR spectra were recorded in $CDCl_3$ or DMSO-d_6 on a Bruker AV-400 spectrometer with tetramethylsilane as the internal standard. A G1313A Standard LC autosampler (Agilent) was used to collect samples for measurement of mass spectra. All reactions were monitored by thin layer chromatography (TLC), and spots were visualized with iodine vapor or by irradiation with UV light. Flash column chromatography was performed on columns packed with silica gel (200−300 mesh). Solvents were of reagent grade and were purified by standard methods when necessary. The purity of compounds was analyzed on a Shimadzu SPD-20A/20AV high-performance liquid chromatography (HPLC) system with a Inertsil ODS-SP, 5 μm C18 column (150 mm × 4.6 mm). HPLC conditions: methanol/water 80:20; flow rate 1.0 mL/min; UV detection from 210 to 400 nm; temperature, ambient; injection volume, 20 μL. The purity of all final compounds was >95%.

*4-((2-Chloropyrimidin-4-yl)oxy)-3,5-dimethylbenzonitrile (**6**).* To a solution of 4-hydroxy-3,5-dimethylbenzonitrile (1.47 g, 10 mmol) and K_2CO_3 (1.70 g, 12 mmol) in DMF (30 mL) was added 2,4-dichloropyrimidine (1.50 g, 10 mmol), and the resultant mixture was stirred at rt for 5 h. The precipitated white solid was collected by filtration, washed with ice−water (100 mL), and recrystallized in DMF−H_2O to provide the intermediate **6** as a white solid in 90% yield. ^{1}H NMR (400 MHz, DMSO-d_6): δ 8.70 (d, J = 5.7 Hz, 1H), 7.75 (s, 2H), 7.32 (d, J = 5.7 Hz, 1H), 2.10 (s, 6H). ESI-MS m/z: 260.3 $[M + H]^+$. $C_{13}H_{10}ClN_3O$ (259.05).

*tert-Butyl-4-((4-(4-cyano-2,6-dimethylphenoxy)pyrimidin-2-yl)-amino)piperidine-1-carboxylate (**7**).* A solution of **6** (0.26 g, 1.0 mmol), *N*-Boc-4-aminopiperidine (0.24 g, 1.2 mmol), and anhydrous K_2CO_3 (0.28 g, 2 mmol) in DMF (5 mL) was heated at 120 °C for 12 h under magnetic stirring. Then, the mixture was cooled to rt and ice−water (40 mL) was added. The resulting precipitate was collected by filtration and dried to give a crude product, which was recrystallized from ethyl acetate (EA)/petroleum ether (PE) to afford the target compound **7** as a white solid in 69% yield. ^{1}H NMR (400 MHz, DMSO-d_6): δ 8.20 (d, J = 5.5 Hz, 1H), 7.68 (s, 2H), 6.39−6.01 (m, 1H), 3.85 (s, 3H), 2.81 (dd, J = 63.9, 1.4 Hz, 3H), 2.08 (s, 6H), 1.64 (d, J = 80.2 Hz, 2H), 1.38 (d, J = 1.5 Hz, 9H), 1.23 (s, 2H). ESI-MS m/z: 424.5 $[M + H]^+$, 446.06 $[M + Na]^+$. $C_{23}H_{29}N_5O_3$ (423.23). HPLC purity: 99.28%.

*tert-Butyl-4-((4-(4-cyano-2,6-dimethylphenoxy)-5-iodopyrimidin-2-yl)amino)piperidine-1-carboxylate (**8**).* Intermediate **7** (0.42 g, 1.0 mmol) was added to a suspension of HOAc (0.30 g, 5.0 mmol) and NIS (0.34 g, 1.5 mmol) in acetonitrile (20 mL). The mixture solution was stirred for 4 h at rt; then, 10% Na_2CO_3 (1.06 g, 10.0 mmol) was added, and the mixture was stirred for another 20 min. The obtained solid was filtered and dried to give a crude product, which was recrystallized in EA to afford the target compound **8** as a white solid in 85% yield. ESI-MS m/z: 550.4 $[M + H]^+$. $C_{23}H_{28}IN_5O_3$ (549.12). HPLC purity: 97.26%.

*4-((5-Iodo-2-(piperidin-4-ylamino)pyrimidin-4-yl)oxy)-3,5-dimethylbenzonitrile (**9**).* To a solution of **8** (0.55 g, 1.0 mmol) in DCM (4 mL) was added TFA (0.74 mL, 10 mmol) at rt, and the mixture was stirred for 6 h (monitored by TLC). Then, the reaction solution was alkalized to pH 9 with saturated sodium bicarbonate solution and extracted with DCM. The organic layer was washed with brine, dried over anhydrous Na_2SO_4, filtered, and concentrated under reduced pressure to give **9** as a white solid in 89% yield. ^{1}H NMR (400 MHz, DMSO-d_6): δ 8.73 (s, 1H), 8.46 (s, 1H, C_6−pyrimidine−H), 7.70 (s, 2H), 7.37 (s, 1H), 3.03−2.97 (m, 2H), 2.09 (d, 6H), 1.97−1.37 (m, 7H). ESI-MS m/z: 450.3 $[M + H]^+$. $C_{18}H_{20}IN_5O$ (449.07). HPLC purity: 96.65%.

https://doi.org/10.1021/acs.jmedchem.1c00268
J. Med. Chem. 2021, 64, 4239−4256

General Procedure for the Preparation of Intermediates 10a−c. To a solution of **9** (0.45 g, 1.0 mmol) in anhydrous DMF (10 mL) were added anhydrous K_2CO_3 (0.28 g, 2.0 mmol) and substituted benzyl chloride (bromine) (1.2 mmol), and the solution was stirred for 4−7 h (monitored by TLC) at rt. The solvent was removed under reduced pressure, and 30 mL of water was added to the residue. Then, the mixture solution was extracted with EA and washed with saturated sodium chloride, purified by flash column chromatography, and recrystallized from EA/PE to afford the target compounds **10a−c**.

*4-((4-((4-(4-Cyano-2,6-dimethylphenoxy)-5-iodopyrimidin-2-yl)-amino)piperidin-1-yl)methyl)benzenesulfonamide (**10a**).* White solid, 76% yield, mp 145−147 °C. ^{1}H NMR (400 MHz, DMSO-d_6): δ 8.42 (s, 1H, C_6−pyrimidine−H), 7.77 (d, J = 8.2 Hz, 2H), 7.69 (s, 2H), 7.45 (d, J = 8.1 Hz, 2H), 7.30 (s, 2H), 7.16 (s, 1H), 3.46−3.42 (m, 2H), 2.68 (s, 2H), 2.07 (s, 6H), 1.92−1.17 (m, 7H). ESI-MS m/z: 619.5 $[M + H]^+$. $C_{25}H_{27}IN_6O_3S$ (618.09). HPLC purity: 97.52%.

*4-((5-Iodo-2-((1-(4-(methylsulfonyl)benzyl)piperidin-4-yl)-amino)pyrimidin-4-yl)oxy)-3,5-dimethylbenzonitrile (**10b**).* White solid, 82% yield, mp 152−154 °C. ^{1}H NMR (400 MHz, DMSO-d_6): δ 8.42 (s, 1H, C_6−pyrimidine−H), 7.87 (d, J = 8.0 Hz, 2H), 7.69 (s, 2H), 7.54 (d, J = 8.0 Hz, 2H), 7.16 (s, 1H), 3.50−3.42 (m, 2H), 3.20 (s, 3H), 2.74 (s, 2H), 2.07 (s, 6H), 1.90−1.16 (m, 7H). ESI-MS m/z: 618.4 $[M + H]^+$. $C_{26}H_{28}IN_5O_3S$ (617.10). HPLC purity: 99.02%.

*4-((4-((4-(4-Cyano-2,6-dimethylphenoxy)-5-iodopyrimidin-2-yl)-amino)piperidin-1-yl)methyl)benzamide (**10c**).* White solid, 71% yield, mp 136−138 °C. ^{1}H NMR (400 MHz, DMSO-d_6): δ 8.42 (s, 1H, C_6−pyrimidine−H), 7.81 (d, J = 7.9 Hz, 2H), 7.68 (s, 2H), 7.36−7.28 (m, 4H), 7.15 (s, 1H), 3.66−3.37 (m, 2H), 2.69 (s, 2H), 2.07 (s, 6H), 1.96−1.17 (m, 7H). ESI-MS m/z: 583.3 $[M + H]^+$. $C_{26}H_{27}IN_6O_2$ (582.12). HPLC purity: 98.65%.

General Procedure for the Preparation of Intermediates 11−16. $Pd(PPh_3)_4$ (0.05 mmol) and 2 M Na_2CO_3 aqueous solution (2.00 mmol) were added to a mixture solution of **10a−c** (1.00 mmol) and boric acid substituents (1.20 mmol) in DMF (10 mL). The mixture was stirred at 100 °C for 6−10 h (monitoring with TLC) under N_2. Then, the mixture was diluted with 10 mL of water, and the aqueous layer was extracted with EtOAc. The organic phase was dried over Na_2SO_4, filtered and evaporated under reduced pressure, purified by flash column chromatography, and recrystallized from EA/PE to afford the target compounds **11−16**.

*4-((4-((4-(4-Cyano-2,6-dimethylphenoxy)-5-(thiophen-2-yl)-pyrimidin-2-yl)amino)piperidin-1-yl)methyl)benzenesulfonamide (**11a**).* **11a** was synthesized from **10a** (602 mg, 1.0 mmol) and thiophen-2-ylboronic acid (153 mg, 1.2 mmol). White solid, 74% yield, mp 152−153 °C. ^{1}H NMR (400 MHz, DMSO-d_6): δ 8.57 (s, 1H, C_6−pyrimidine−H), 7.71 (d, J = 8.0 Hz, 2H, C_3,C_5−Ph−H), 7.63 (s, 2H, C_3,C_5−Ph′−H), 7.52−7.43 (m, 3H), 7.39 (d, J = 8.0 Hz, 2H, C_2,C_6−Ph−H), 7.24 (s, 2H, SO_2NH_2), 7.06−7.05 (m, 1H), 3.42 (s, 2H, N−CH_2), 2.68−2.57 (m, 2H), 2.02 (s, 6H), 1.94−1.15 (m, 7H). ^{13}C NMR (100 MHz, DMSO-d_6): δ 163.3, 160.4, 143.1, 135.3, 133.0, 129.4, 127.8, 126.9, 125.9, 123.9, 119.1, 108.7, 62.7, 61.9, 52.6, 31.3, 16.4. ESI-MS m/z: 575.6 $[M + H]^+$, 597.5 $[M + Na]^+$. $C_{29}H_{30}N_6O_3S_2$ (574.18). HPLC purity: 95.98%.

*3,5-Dimethyl-4-((2-((1-(4-(methylsulfonyl)benzyl)piperidin-4-yl)-amino)-5-(thiophen-2-yl)pyrimidin-4-yl)oxy)benzonitrile (**11b**).* **11b** was synthesized from **10b** (602 mg, 1.0 mmol) and thiophen-2-ylboronic acid (153 mg, 1.2 mmol). White solid, 82% yield, mp 168−170 °C. ^{1}H NMR (400 MHz, DMSO-d_6): δ 8.58 (s, 1H, C_6−pyrimidine−H), 7.81 (d, J = 7.9 Hz, 2H, C_3,C_5−Ph−H), 7.63 (s, 2H, C_3,C_5−Ph′−H), 7.61−7.59 (m, 1H), 7.48 (d, J = 7.8 Hz, 2H, C_2,C_6−Ph−H), 7.42−7.40 (m, 2H), 7.06 (s, 1H), 3.43 (s, 2H, N−CH_2), 3.13 (s, 3H, SO_2CH_3), 2.68−2.60 (m, 2H), 2.02 (s, 6H), 1.94−1.24 (m, 7H). ^{13}C NMR (100 MHz, DMSO-d_6): δ 163.3, 160.5, 145.4, 139.8, 135.3, 133.1, 132.5, 129.8, 127.8, 127.4, 125.4, 123.9, 119.1, 61.8, 52.8, 44.0, 31.3, 16.3. ESI-MS m/z: 574.2 $[M + H]^+$, 596.2 $[M + Na]^+$. $C_{30}H_{31}N_5O_3S_2$ (573.19). HPLC purity: 98.32%.

*4-((4-((4-(4-Cyano-2,6-dimethylphenoxy)-5-(thiophen-2-yl)-pyrimidin-2-yl)amino)piperidin-1-yl)methyl)benzamide (**11c**).* **11c** was synthesized from **10c** (583 mg, 1.0 mmol) and thiophen-2-ylboronic acid (153 mg, 1.2 mmol). White solid, 70% yield, mp 155−157 °C. ^{1}H NMR (400 MHz, DMSO-d_6): δ 8.58 (s, 1H, C_6−pyrimidine−H), 7.85 (s, 1H), 7.75 (d, J = 7.8 Hz, 2H, C_3,C_5−Ph−H), 7.63 (s, 2H, C_3,C_5−Ph′−H), 7.48−7.45 (m, 2H), 7.27 (d, J = 7.8 Hz, 2H, C_2,C_6−Ph−H), 7.23 (s, 2H, $CONH_2$), 7.06 (s, 1H), 3.38 (s, 2H, N−CH_2), 2.68−2.59 (m, 2H), 2.03 (s, 6H), 1.94−1.15 (m, 7H). ^{13}C NMR (100 MHz, DMSO-d_6): δ 168.2, 163.3, 160.4, 142.4, 135.3, 133.4, 133.0, 132.6, 128.9, 127.9, 125.5, 124.0, 121.5, 120.4, 119.1, 108.7, 62.1, 52.7, 31.7, 29.1, 16.3. ESI-MS m/z: 539.7 $[M + H]^+$, 561.1 $[M + Na]^+$. $C_{30}H_{30}N_6O_2S$ (538.22). HPLC purity: 98.29%.

*4-((4-((4-(4-Cyano-2,6-dimethylphenoxy)-5-(thiophen-3-yl)-pyrimidin-2-yl)amino)piperidin-1-yl)methyl)benzenesulfonamide (**12a**).* **12a** was synthesized from **10a** (602 mg, 1.0 mmol) and thiophen-3-ylboronic acid (153 mg, 1.2 mmol). White solid, 72% yield, mp 144−146 °C. ^{1}H NMR (400 MHz, DMSO-d_6): δ 8.60 (s, 1H, C_6−pyrimidine−H), 7.78 (d, J = 8.0 Hz, 2H, C_3,C_5−Ph−H), 7.67 (s, 2H, C_3,C_5−Ph′−H), 7.62 (s, 2H), 7.46 (d, J = 8.0 Hz, 2H, C_2,C_6−Ph−H), 7.35−7.30 (m, 3H), 7.02 (s, 1H, NH), 3.47 (s, 2H, N−CH_2), 2.78−2.61 (m, 2H), 2.08 (s, 6H), 1.85−1.10 (m, 7H). ^{13}C NMR (100 MHz, DMSO-d_6): δ 164.3, 155.0, 143.3, 133.8, 133.0, 129.4, 126.6, 126.0, 119.1, 108.5, 104.4, 61.9, 60.2, 52.6, 21.2, 16.3, 14.5. ESI-MS m/z: 575.5 $[M + H]^+$, 597.3 $[M + Na]^+$. $C_{29}H_{30}N_6O_3S_2$ (574.18). HPLC purity: 99.11%.

*3,5-Dimethyl-4-((2-((1-(4-(methylsulfonyl)benzyl)piperidin-4-yl)-amino)-5-(thiophen-3-yl)pyrimidin-4-yl)oxy)benzonitrile (**12b**).* **12b** was synthesized from **10b** (602 mg, 1.0 mmol) and thiophen-3-ylboronic acid (153 mg, 1.2 mmol). White solid, 66% yield, mp 159−161 °C. ^{1}H NMR (400 MHz, DMSO-d_6): δ 8.60 (s, 1H, C_6−pyrimidine−H), 7.88 (d, J = 7.9 Hz, 2H, C_3,C_5−Ph−H), 7.83−7.68 (m, 1H), 7.62 (s, 2H, C_3,C_5−Ph′−H), 7.67−7.60 (m, 2H), 7.55 (d, J = 8.0 Hz, 2H, C_2,C_6−Ph−H), 7.02 (s, 1H, NH), 3.43 (s, 2H, N−CH_2), 3.20 (s, 3H, SO_2CH_3), 2.86−2.58 (m, 2H), 2.08 (s, 6H), 1.94−1.17 (m, 7H). ^{13}C NMR (100 MHz, DMSO-d_6): δ 164.1, 155.2, 145.1, 143.6, 139.0, 133.3, 132.4, 129.7, 127.8, 119.1, 118.2, 108.6, 61.9, 52.7, 44.0, 31.3, 16.2. ESI-MS m/z: 574.3 $[M + H]^+$, 596.6 $[M + Na]^+$. $C_{30}H_{31}N_5O_3S_2$ (573.19). HPLC purity: 98.66%.

*4-((4-((4-(4-Cyano-2,6-dimethylphenoxy)-5-(thiophen-3-yl)-pyrimidin-2-yl)amino)piperidin-1-yl)methyl)benzamide (**12c**).* **12c** was synthesized from **10c** (583 mg, 1.0 mmol) and thiophen-3-ylboronic acid (153 mg, 1.2 mmol). White solid, 74% yield, mp 140−142 °C. ^{1}H NMR (400 MHz, DMSO-d_6): δ 8.60 (s, 1H, C_6−pyrimidine−H), 7.92 (s, 1H), 7.82 (d, J = 8.0 Hz, 2H, C_3,C_5−Ph−H), 7.68 (s, 2H, C_3,C_5−Ph′−H), 7.62 (s, 2H), 7.33 (d, J = 7.9 Hz, 2H, C_2,C_6−Ph−H), 7.30 (s, 2H, $CONH_2$), 7.02 (s, 1H), 3.44 (s, 2H, N−CH_2), 2.64−2.59 (m, 2H), 2.09 (s, 6H), 2.00−1.20 (m, 7H). ^{13}C NMR (100 MHz, DMSO-d_6): δ 164.2, 155.0, 143.7, 140.2, 133.1, 131.9, 129.1, 126.5, 122.8, 121.4, 119.8, 118.2, 115.8, 108.0, 61.9, 60.2, 52.5, 21.2, 16.3, 14.5. ESI-MS m/z: 539.4 $[M + H]^+$, 561.3 $[M + Na]^+$. $C_{30}H_{30}N_6O_2S$ (538.22). HPLC purity: 96.59%.

*4-((4-((4-(4-Cyano-2,6-dimethylphenoxy)-5-(furan-2-yl)-pyrimidin-2-yl)amino)piperidin-1-yl)methyl)benzenesulfonamide (**13a**).* **13a** was synthesized from **10a** (602 mg, 1.0 mmol) and furan-2-ylboronic acid (134 mg, 1.2 mmol). White solid, 77% yield, mp 140−142 °C. ^{1}H NMR (400 MHz, DMSO-d_6): δ 8.61 (s, 1H, C_6−pyrimidine−H), 7.78 (d, J = 7.9 Hz, 2H, C_3,C_5−Ph−H), 7.77−7.70 (m, 2H), 7.72 (s, 2H, C_3,C_5−Ph′−H), 7.46 (d, J = 8.0 Hz, 2H, C_2,C_6−Ph−H), 7.31−7.19 (m, 3H), 6.59 (s, 1H, NH), 3.47 (s, 2H, N−CH_2), 2.51−2.02 (m, 2H), 2.02 (s, 6H), 1.95−1.13 (m, 7H). ^{13}C NMR (100 MHz, DMSO-d_6): δ 170.8, 163.0, 160.2, 156.3, 147.1, 143.2, 142.1, 133.1, 129.4, 126.9, 126.0, 119.1, 112.3, 108.7, 61.9, 60.2, 52.7, 21.2, 16.1. ESI-MS m/z: 559.4 $[M + H]^+$, 581.4 $[M + Na]^+$. $C_{29}H_{30}N_6O_4S$ (558.20). HPLC purity: 98.96%.

*4-((5-(Furan-2-yl)-2-((1-(4-(methylsulfonyl)benzyl)piperidin-4-yl)amino)pyrimidin-4-yl)oxy)-3,5-dimethylbenzonitrile (**13b**).* **13b** was synthesized from **10b** (602 mg, 1.0 mmol) and furan-2-ylboronic acid (134 mg, 1.2 mmol). White solid, 82% yield, mp 137−139 °C. ^{1}H NMR (400 MHz, DMSO-d_6): δ 8.60 (s, 1H, C_6−pyrimidine−H), 7.88 (d, J = 7.9 Hz, 2H, C_3,C_5−Ph−H), 7.72−7.63 (m, 3H), 7.55 (d, J = 7.8 Hz, 2H, C_2,C_6−Ph−H), 6.73 (d, J = 11.7 Hz, 1H), 7.21−7.19

https://doi.org/10.1021/acs.jmedchem.1c00268
J. Med. Chem. 2021, 64, 4239−4256

(m, 1H), 6.59 (s, 1H, NH), 3.51 (s, 2H, N−CH_2), 3.20 (s, 3H, SO_2CH_3), 2.83−2.57 (m, 2H), 2.02 (s, 6H), 1.94−1.18 (m, 7H). ^{13}C NMR (100 MHz, DMSO-d_6): δ 163.0, 160.3, 156.0, 147.1, 145.3, 142.1, 139.8, 133.1, 132.5, 129.8, 128.5, 127.4, 119.1, 112.3, 107.7, 61.8, 52.7, 44.0, 31.2, 16.3. ESI-MS *m/z*: 558.6 $[M + H]^+$, 580.4 $[M + Na]^+$. $C_{30}H_{31}N_5O_4S$ (557.21). HPLC purity: 97.52%.

*4-((4-((4-(4-Cyano-2,6-dimethylphenoxy)-5-(furan-2-yl)-pyrimidin-2-yl)amino)piperidin-1-yl)methyl)benzamide (**13c**).* **13c** was synthesized from **10c** (583 mg, 1.0 mmol) and furan-2-ylboronic acid (134 mg, 1.2 mmol). White solid, 65% yield, mp 148−150 °C. ^{1}H NMR (400 MHz, DMSO-d_6): δ 8.60 (s, 1H, C_6−pyrimidine−H), 7.91 (s, 1H), 7.82 (d, *J* = 7.8 Hz, 2H, C_3,C_5−Ph−H), 7.71 (s, 2H, C_3,C_5−Ph′−H), 7.52 (s, 1H), 7.41−7.14 (m, 4H), 6.73 (d, *J* = 12.4 Hz, 1H), 6.58 (s, 1H, NH), 3.38 (s, 2H, N−CH_2), 2.89−2.60 (m, 2H), 2.03 (s, 6H), 1.94−1.14 (m, 7H). ^{13}C NMR (100 MHz, DMSO-d_6): δ 168.2, 163.0, 160.2, 154.2, 147.1, 142.1, 133.4, 133.0, 132.5, 128.9, 127.9, 119.1, 112.3, 108.7, 100.6, 62.1, 52.5, 31.2, 16.0. ESI-MS *m/z*: 523.3 $[M + H]^+$. $C_{30}H_{30}N_6O_3$ (522.24). HPLC purity: 97.49%.

*4-((4-((4-(4-Cyano-2,6-dimethylphenoxy)-5-(furan-3-yl)-pyrimidin-2-yl)amino)piperidin-1-yl)methyl)benzenesulfonamide (**14a**).* **14a** was synthesized from **10a** (602 mg, 1.0 mmol) and furan-3-ylboronic acid (134 mg, 1.2 mmol). White solid, 69% yield, mp 172−174 °C. ^{1}H NMR (400 MHz, DMSO-d_6): δ 8.52 (s, 1H, C_6−pyrimidine−H), 8.00 (s, 1H), 7.85 (s, 1H), 7.75 (d, *J* = 7.8 Hz, 2H, C_3,C_5−Ph−H), 7.68 (s, 1H), 7.62 (s, 2H, C_3,C_5−Ph′−H), 7.30−7.19 (m, 4H), 7.00 (s, 1H, NH), 3.39−3.32 (m, 2H, N−CH_2), 2.77−2.52 (m, 2H), 2.01 (s, 6H), 1.81−1.07 (m, 7H). ^{13}C NMR (100 MHz, DMSO-d_6): δ 168.2, 164.2, 160.4, 143.9, 140.0, 133.4, 133.1, 132.6, 128.9, 127.9, 126.0, 119.1, 118.2, 108.9, 108.5, 62.1, 52.6, 39.4, 31.4, 16.2. ESI-MS *m/z*: 559.3 $[M + H]^+$, 581.4 $[M + Na]^+$. $C_{29}H_{30}N_6O_4S$ (558.20). HPLC purity: 98.96%.

*4-((5-(Furan-3-yl)-2-((1-(4-(methylsulfonyl)benzyl)piperidin-4-yl)amino)pyrimidin-4-yl)oxy)-3,5-dimethylbenzonitrile (**14b**).* **14b** was synthesized from **10b** (602 mg, 1.0 mmol) and furan-3-ylboronic acid (134 mg, 1.2 mmol). White solid, 77% yield, mp 180−182 °C. ^{1}H NMR (400 MHz, DMSO-d_6): δ 8.52 (s, 1H, C_6−pyrimidine−H), 8.01 (s, 1H), 7.81 (d, *J* = 7.9 Hz, 2H, C_3,C_5−Ph−H), 7.70−7.66 (m, 1H), 7.62 (s, 2H, C_3,C_5−Ph′−H), 7.48 (d, *J* = 7.9 Hz, 2H, C_2,C_6−Ph−H), 7.27 (s, 1H), 7.00 (s, 1H, NH), 3.44 (s, 2H, N−CH_2), 3.13 (s, 3H, SO_2CH_3), 2.75−2.63 (m, 2H), 2.01 (s, 6H), 1.90−1.28 (m, 7H). ^{13}C NMR (100 MHz, DMSO-d_6): δ 164.2, 145.4, 143.9, 140.0, 139.8, 133.1, 132.6, 129.7, 127.4, 119.1, 118.2, 108.8, 61.9, 52.7, 44.0, 31.4, 16.2. ESI-MS *m/z*: 558.5 $[M + H]^+$, 580.2 $[M + Na]^+$. $C_{30}H_{31}N_5O_4S$ (557.21). HPLC purity: 99.01%.

*4-((4-((4-(4-Cyano-2,6-dimethylphenoxy)-5-(furan-3-yl)-pyrimidin-2-yl)amino)piperidin-1-yl)methyl)benzamide (**14c**).* **14c** was synthesized from **10c** (583 mg, 1.0 mmol) and furan-3-ylboronic acid (134 mg, 1.2 mmol). White solid, 71% yield, mp 158−160 °C. ^{1}H NMR (400 MHz, DMSO-d_6): δ 8.52 (s, 1H, C_6−pyrimidine−H), 8.00 (s, 1H), 7.76−7.68 (m, 4H), 7.62 (s, 2H), 7.39 (d, *J* = 7.9 Hz, 2H, C_2,C_6−Ph−H), 7.24 (s, 2H), 7.00 (s, 1H, NH), 3.39 (s, 2H, N−CH_2), 2.81−2.53 (m, 2H), 2.01 (s, 6H), 1.96−1.19 (m, 7H). ^{13}C NMR (100 MHz, DMSO-d_6): δ 164.2, 143.9, 143.1, 140.0, 133.1, 132.4, 129.4, 126.0, 123.0, 121.9, 119.1, 118.2, 115.8, 108.8, 61.9, 60.2, 52.6, 21.2, 16.2, 14.5. ESI-MS *m/z*: 523.3 $[M + H]^+$, 545.4 $[M + Na]^+$. $C_{30}H_{30}N_6O_3$ (522.24). HPLC purity: 97.48%.

*4-((4-((4-(4-Cyano-2,6-dimethylphenoxy)-5-phenylpyrimidin-2-yl)amino)piperidin-1-yl)methyl)benzenesulfonamide (**15a**).* **15a** was synthesized from **10a** (602 mg, 1.0 mmol) and phenylboronic acid (145 mg, 1.2 mmol). White solid, 79% yield, mp 162−164 °C. ^{1}H NMR (400 MHz, DMSO-d_6): δ 8.34 (s, 1H, C_6−pyrimidine−H), 7.78 (d, *J* = 8.0 Hz, 2H, C_3,C_5−Ph−H), 7.64 (s, 2H, C_3,C_5−Ph′−H), 7.64−7.49 (m, 3H), 7.45−7.39 (m, 3H), 7.32 (d, *J* = 8.0 Hz, 2H, C_2,C_6−Ph−H), 7.05 (s, 1H), 3.47 (s, 2H, N−CH_2), 2.89−2.59 (m, 2H), 2.08 (s, 6H), 1.87−1.15 (m, 7H). ^{13}C NMR (100 MHz, DMSO): δ 164.7, 161.0, 156.2, 154.4, 143.4, 143.1, 133.0, 132.5, 129.4, 129.0, 128.6, 127.3, 126.0, 119.1, 115.7, 112.4, 108.6, 62.0, 60.2, 52.7, 21.2, 16.4, 14.5. ESI-MS *m/z*: 569.2 $[M + H]^+$. $C_{31}H_{32}N_6O_3S$ (568.23). HPLC purity: 96.98%.

*3,5-Dimethyl-4-((2-((1-(4-(methylsulfonyl)benzyl)piperidin-4-yl)-amino)-5-phenylpyrimidin-4-yl)oxy)benzonitrile (**15b**).* **15b** was synthesized from **10b** (602 mg, 1.0 mmol) and phenylboronic acid (145 mg, 1.2 mmol). White solid, 81% yield, mp 147−149 °C. ^{1}H NMR (400 MHz, DMSO-d_6): δ 8.27 (s, 1H, C_6−pyrimidine−H), 7.81 (d, *J* = 8.0 Hz, 2H, C_3,C_5−Ph−H), 7.64−7.53 (m, 4H), 7.48 (d, *J* = 7.9 Hz, 2H, C_2,C_6−Ph−H), 7.38 (t, *J* = 7.7 Hz, 2H), 7.26 (t, *J* = 7.6 Hz, 1H), 6.97 (s, 1H), 3.54−3.35 (m, 2H, N−CH_2), 3.13 (s, 3H, SO_2CH_3), 2.68−2.62 (m, 2H), 2.01 (s, 6H), 1.90−1.17 (m, 7H). ^{13}C NMR (100 MHz, DMSO): δ 164.3, 156.0, 153.8, 143.7, 142.8, 133.7, 132.5, 129.0, 128.6, 127.3, 125.2, 118.4, 115.6, 112.7, 108.0, 62.1, 52.7, 21.4, 16.3, 14.5. ESI-MS *m/z*: 568.4 $[M + H]^+$, 590.5 $[M + Na]^+$. $C_{32}H_{33}N_5O_3S$ (567.23). HPLC purity: 98.59%.

*4-((4-((4-(4-Cyano-2,6-dimethylphenoxy)-5-phenylpyrimidin-2-yl)amino)piperidin-1-yl)methyl)benzamide (**15c**).* **15c** was synthesized from **10c** (583 mg, 1.0 mmol) and phenylboronic acid (145 mg, 1.2 mmol). White solid, 64% yield, mp 150−152 °C. ^{1}H NMR (400 MHz, DMSO-d_6): δ 8.34 (s, 1H, C_6−pyrimidine−H), 7.92 (s, 1H), 7.83 (d, *J* = 7.8 Hz, 2H, C_3,C_5−Ph−H), 7.65 (d, *J* = 12.5 Hz, 4H), 7.45 (t, *J* = 7.6 Hz, 2H), 7.37−7.27 (m, 4H), 7.04 (s, 1H, NH), 3.38 (s, 2H, N−CH_2), 2.73−2.57 (m, 2H), 2.08 (s, 6H), 2.02−1.17 (m, 7H). ^{13}C NMR (100 MHz, DMSO-d_6): δ 164.2, 155.7, 152.6, 143.7, 142.4, 133.1, 131.7, 129.3, 125.8, 122.3, 119.3, 118.2, 115.8, 108.0, 61.7, 60.2, 52.5, 21.2, 16.4, 14.5. ESI-MS *m/z*: 533.7 $[M + H]^+$, 555.2 $[M + Na]^+$. $C_{32}H_{32}N_6O_2$ (532.26). HPLC purity: 98.96%.

*4-((4-((4-(4-Cyano-2,6-dimethylphenoxy)-5-(pyridin-4-yl)-pyrimidin-2-yl)amino)piperidin-1-yl)methyl)benzenesulfonamide (**16a**).* **16a** was synthesized from **10a** (602 mg, 1.0 mmol) and pyridin-4-ylboronic acid (145 mg, 1.2 mmol). White solid, 53% yield, mp 174−176 °C. ^{1}H NMR (400 MHz, DMSO-d_6): δ 8.60−8.54 (m, 3H), 8.18 (d, *J* = 5.4 Hz, 2H), 7.76−7.73 (m, 2H), 7.64 (s, 2H, C_3,C_5−Ph′−H), 7.46 (d, *J* = 8.0 Hz, 2H), 7.31 (s, 2H), 6.95 (s, 1H, NH), 3.47 (s, 2H, N−CH_2), 2.87−2.59 (m, 2H), 2.09 (s, 6H), 2.03−1.22 (m, 7H). ^{13}C NMR (100 MHz, DMSO): δ 164.5, 161.4, 156.4, 143.7, 143.0, 133.6, 129.4, 129.0, 128.5, 128.1, 127.3, 126.2, 119.0, 118.2, 115.7, 112.9, 108.3, 62.0, 60.7, 52.7, 21.2, 16.4, 14.5. ESI-MS *m/z*: 570.3 $[M + H]^+$, 592.1 $[M + Na]^+$. $C_{30}H_{31}N_7O_3S$ (569.22). HPLC purity: 99.32%.

*3,5-Dimethyl-4-((2-((1-(4-(methylsulfonyl)benzyl)piperidin-4-yl)-amino)-5-(pyridin-4-yl)pyrimidin-4-yl)oxy)benzonitrile (**16b**).* **16b** was synthesized from **10b** (602 mg, 1.0 mmol) and pyridin-4-ylboronic acid (145 mg, 1.2 mmol). White solid, 59% yield, mp 158−160 °C. ^{1}H NMR (400 MHz, DMSO-d_6): δ 8.60 (d, *J* = 5.1 Hz, 2H), 8.55 (d, *J* = 6.2 Hz, 1H), 7.88 (d, *J* = 7.9 Hz, 2H), 7.74 (d, *J* = 5.1 Hz, 1H), 7.69 (s, 3H), 7.55 (d, *J* = 7.9 Hz, 2H), 7.04 (s, 1H), 3.55−3.48 (m, 2H, N−CH_2), 3.20 (s, 3H), 2.92−2.60 (m, 2H), 2.09 (s, 6H), 2.02−1.22 (m, 7H). ^{13}C NMR (100 MHz, DMSO): δ 164.2, 160.7, 156.9, 153.8, 143.7, 142.1, 133.7, 132.5, 128.2, 127.9, 125.8, 119.3, 118.3, 115.0, 112.7, 108.0, 62.3, 52.7, 21.4, 16.4, 14.5. ESI-MS *m/z*: 569.2 $[M + H]^+$, 591.5 $[M + Na]^+$. $C_{31}H_{32}N_6O_3S$ (568.23). HPLC purity: 97.65%.

*4-((4-((4-(4-Cyano-2,6-dimethylphenoxy)-5-(pyridin-4-yl)-pyrimidin-2-yl)amino)piperidin-1-yl)methyl)benzamide (**16c**).* **16c** was synthesized from **10c** (583 mg, 1.0 mmol) and pyridin-4-ylboronic acid (145 mg, 1.2 mmol). White solid, 52% yield, mp 163−165 °C. ^{1}H NMR (400 MHz, DMSO-d_6): δ 8.61−8.53 (m, 3H), 7.87 (d, *J* = 7.8 Hz, 2H), 7.74−7.67 (m, 4H), 7.69 (s, 2H), 7.55 (d, *J* = 7.9 Hz, 2H), 7.04 (s, 1H), 3.50−3.48 (m, 2H, N−CH_2), 2.75−2.61 (m, 2H), 2.08 (s, 6H), 2.02−1.29 (m, 7H). ^{13}C NMR (100 MHz, DMSO-d_6): δ 164.3, 160.1, 155.8, 152.6, 143.6, 142.3, 133.7, 132.1, 129.2, 127.4, 125.1, 122.2, 119.0, 118.5, 115.8, 108.7, 61.5, 60.2, 52.5, 21.2, 16.4, 14.5. ESI-MS *m/z*: 534.7 $[M + H]^+$, 556.4 $[M + Na]^+$. $C_{31}H_{31}N_7O_2$ (533.25). HPLC purity: 98.78%.

*(E)-3-(4-((2-Chloropyrimidin-4-yl)oxy)-3,5-dimethylphenyl)-acrylonitrile (**17**).* The synthetic method was similar to that described for **6**, except that the starting material **5** (1.50 g, 10 mmol) was reacted with (*E*)-3-(4-hydroxy-3,5-dimethylphenyl)acrylonitrile (2.07 g, 12 mmol). White solid, 84% yield. ^{1}H NMR (400 MHz, DMSO-d_6): δ 8.67 (d, *J* = 5.7 Hz, 1H), 7.62 (d, *J* = 16.7 Hz, 1H), 7.52 (s, 2H), 7.25 (d, *J* = 5.7 Hz, 1H), 6.45 (d, *J* = 16.7 Hz, 1H), 2.07 (s, 6H).

https://doi.org/10.1021/acs.jmedchem.1c00268
J. Med. Chem. 2021, 64, 4239−4256

ESI-MS m/z: 286.2 $[M + H]^+$. $C_{15}H_{12}ClN_3O$ (285.07). HPLC purity: 98.39%.

*tert-Butyl(E)-4-((4-(4-(2-cyanovinyl)-2,6-dimethylphenoxy)-pyrimidin-2-yl)amino)piperidine-1-carboxylate (**18**).* The synthetic method was similar to that described for **7**, except that the starting material **17** (0.28 g, 1.0 mmol) was reacted with *N*-Boc-4-aminopiperidine (0.24 g, 1.2 mmol). White solid, 70% yield. ^1H NMR (400 MHz, DMSO-d_6): δ 8.17 (d, J = 5.6 Hz, 1H), 7.68−7.51 (m, 1H), 7.46 (d, J = 4.5 Hz, 2H), 6.40 (d, J = 16.6 Hz, 1H), 6.17 (s, 1H), 3.85 (s, 3H), 2.81 (d, J = 63.8 Hz, 2H), 2.06 (s, 6H), 1.91−1.52 (m, 3H), 1.41 (d, J = 6.0 Hz, 3H), 1.38 (s, 6H), 1.31−0.99 (m, 2H). ESI-MS m/z: 472.02 $[M + Na]^+$. $C_{25}H_{31}N_5O_3$ (449.24). HPLC purity: 98.79%.

*tert-Butyl(E)-4-((4-(4-(2-cyanovinyl)-2,6-dimethylphenoxy)-5-iodopyrimidin-2-yl)amino)piperidine-1-carboxylate (**19**).* The synthetic method was similar to that described for **8**, except that NIS (0.34 g, 1.5 mmol) was reacted with **18** (0.47 g, 1.0 mmol). White solid, 79% yield. ESI-MS m/z: 576.2 $[M + H]^+$. $C_{25}H_{30}IN_5O_3$ (575.14). HPLC purity: 96.28%.

*(E)-3-(4-((5-Iodo-2-(piperidin-4-ylamino)pyrimidin-4-yl)oxy)-3,5-dimethylphenyl)acrylonitrile (**20**).* The synthetic method was similar to that described for **9**. White solid, 85% yield. ^1H NMR (400 MHz, DMSO-d_6): δ 8.45 (s, 1H, C_6−pyrimidine−H), 8.27 (s, 1H), 7.60 (d, J = 16.6 Hz, 1H, ArCH═), 7.47 (s, 2H), 7.32 (d, J = 13.5 Hz, 1H), 6.42 (d, J = 16.7 Hz, 1H, ═CHCN), 3.23−2.71 (m, 5H), 2.06 (s, 6H), 1.94−1.26 (m, 4H). ESI-MS m/z: 476.2 $[M + H]^+$, 498.5 $[M + Na]^+$. $C_{20}H_{22}IN_5O$ (475.09). HPLC purity: 97.09%.

*(E)-4-((4-((4-(4-(2-Cyanovinyl)-2,6-dimethylphenoxy)-5-iodopyrimidin-2-yl)amino)piperidin-1-yl)methyl)benzenesulfonamide (**21a**).* The synthetic method was similar to that described for **10a−c**. White solid, 75% yield, mp: 210−212 °C. ^1H NMR (400 MHz, DMSO-d_6): δ 8.41 (s, 1H, C_6−pyrimidine−H), 7.96 (s, 1H), 7.77 (d, J = 7.9 Hz, 2H), 7.68−7.55 (m, 2H), 7.46 (s, 2H), 7.35−7.26 (m, 2H), 7.15 (s, 1H, NH), 6.42 (d, J = 16.7 Hz, 1H, ═CHCN), 3.41 (s, 2H, N−CH_2), 2.74 (s, 2H), 2.04 (s, 6H), 1.86−1.08 (m, 7H). ESI-MS m/z: 645.7 $[M + H]^+$, 667.2 $[M + Na]^+$. $C_{27}H_{29}IN_6O_3S$ (644.11). HPLC purity: 96.59%.

*(E)-3-(4-((5-Iodo-2-((1-(4-(methylsulfonyl)benzyl)piperidin-4-yl)-amino)pyrimidin-4-yl)oxy)-3,5-dimethylphenyl)acrylonitrile (**21b**).* The synthetic method was similar to that described for **10a−c**. White solid, 82% yield, mp: 204−206 °C. ^1H NMR (400 MHz, DMSO-d_6): δ 8.41 (s, 1H, C_6−pyrimidine−H), 7.88 (d, J = 8.1 Hz, 2H), 7.68−7.58 (m, 2H), 7.45 (s, 2H), 7.29−7.27 (m, 1H), 7.15 (s, 1H, NH), 6.41 (d, J = 16.7 Hz, 1H, ═CHCN), 3.47−3.45 (m, 2H), 3.20 (s, 3H, SO_2CH_3), 2.74 (s, 2H), 2.04 (s, 6H), 1.83−1.10 (m, 7H). ESI-MS m/z: 644.5 $[M + H]^+$, 666.3 $[M + Na]^+$. $C_{28}H_{30}IN_5O_3S$ (643.11). HPLC purity: 99.02%.

*(E)-4-((4-((4-(4-(2-Cyanovinyl)-2,6-dimethylphenoxy)-5-iodopyrimidin-2-yl)amino)piperidin-1-yl)methyl)benzamide (**21c**).* The synthetic method was similar to that described for **10a−c**. White solid, 74% yield, mp: 231−232 °C. ^1H NMR (400 MHz, DMSO-d_6): δ 8.40 (s, C_6−pyrimidine−H), 7.91 (s, 1H), 7.81 (d, J = 7.9 Hz, 2H), 7.45 (s, 2H), 7.38−7.08 (m, 5H), 6.42 (d, J = 16.5 Hz, 1H, ═CHCN), 3.54−3.47 (m, 2H), 2.74 (s, 2H), 2.04 (s, 6H), 1.99−1.21 (m, 7H). ESI-MS m/z: 609.2 $[M + H]^+$, 631.4 $[M + Na]^+$. $C_{28}H_{29}IN_6O_2$ (608.14). HPLC purity: 99.25%.

*(E)-4-((4-((4-(4-(2-Cyanovinyl)-2,6-dimethylphenoxy)-5-(pyridin-4-yl)pyrimidin-2-yl)amino)piperidin-1-yl)methyl)-benzenesulfonamide (**22a**).* **22a** was synthesized from **21a** (644 mg, 1.0 mmol) and pyridin-4-ylboronic acid (145 mg, 1.2 mmol). White solid, 59% yield, mp: 134−136 °C. ^1H NMR (400 MHz, DMSO-d_6): δ 8.53 (s, 1H, C_6−pyrimidine−H), 8.46 (d, J = 6.6 Hz, 2H), 7.71 (d, J = 8.1 Hz, 2H), 7.65−7.47 (m, 3H), 7.39−7.35 (m, 3H), 7.24−7.21 (m, 3H), 6.91 (s, 1H, NH), 6.35 (d, J = 17.3 Hz, 1H, ═CHCN), 3.43 (s, 2H, N−CH_2), 2.88−2.47 (m, 2H), 1.99 (s, 6H), 1.87−1.09 (m, 7H). ^{13}C NMR (100 MHz, DMSO-d_6): δ 170.6, 165.3, 161.6, 160.4, 150.7, 150.4, 143.2, 131.6, 129.5, 128.6, 128.1, 126.0, 123.0, 122.5, 119.4, 96.6, 90.8, 62.1, 52.8, 50.6, 31.6, 29.0, 16.5. ESI-MS m/z: 596.3 $[M + H]^+$, 618.5 $[M + Na]^+$. $C_{32}H_{33}N_7O_3S$ (595.24). HPLC purity: 97.19%.

*(E)-3-(3,5-Dimethyl-4-((2-((1-(4-(methylsulfonyl)benzyl)-piperidin-4-yl)amino)-5-(pyridin-4-yl)pyrimidin-4-yl)oxy)phenyl)-acrylonitrile (**22b**).* **22b** was synthesized from **21b** (643 mg, 1.0 mmol) and pyridin-4-ylboronic acid (145 mg, 1.2 mmol). White solid, 63% yield, mp: 122−124 °C. ^1H NMR (400 MHz, DMSO-d_6): δ 8.75−8.47 (m, 3H), 7.88 (d, J = 7.8 Hz, 2H), 7.75−7.69 (m, 2H), 7.66−7.49 (m, 3H), 7.46 (s, 2H), 6.91 (s, 1H, NH), 6.41 (d, J = 16.9 Hz, 1H, ═CHCN), 3.48−3.45 (m, 2H, N−CH_2), 3.20 (s, 3H, SO_2CH_3), 2.94−2.54 (m, 2H), 2.07 (s, 6H), 2.00−1.17 (m, 7H). ^{13}C NMR (100 MHz, DMSO-d_6): δ 168.8, 165.2, 161.5, 150.6, 150.2, 145.5, 139.8, 131.6, 131.3, 129.7, 128.6, 128.2, 127.4, 122.6, 119.4, 105.6, 61.9, 52.8, 44.0, 31.7, 29.0, 16.6. ESI-MS m/z: 595.5 $[M + H]^+$. $C_{33}H_{34}N_6O_3S$ (594.2). HPLC purity: 98.54%.

*(E)-4-((4-((4-(4-(2-Cyanovinyl)-2,6-dimethylphenoxy)-5-(pyridin-4-yl)pyrimidin-2-yl)amino)piperidin-1-yl)methyl)benzamide (**22c**).* **22c** was synthesized from **21c** (608 mg, 1.0 mmol) and pyridin-4-ylboronic acid (145 mg, 1.2 mmol). White solid, 50% yield, mp: 125−127 °C. ^1H NMR (400 MHz, DMSO-d_6): δ 8.52 (s, 1H, C_6−pyrimidine−H), 8.46 (d, J = 6.0 Hz, 2H), 7.85 (s, 1H), 7.76 (d, J = 7.7 Hz, 2H), 7.70−7.47 (m, 3H), 7.39 (s, 2H), 7.32−7.18 (m, 3H), 6.90 (s, 1H, NH), 6.34 (d, J = 16.7 Hz, 1H, ═CHCN), 3.41 (s, 2H, N−CH_2), 2.73 (s, 2H), 1.99 (s, 6H), 1.77−1.15 (m, 7H). ^{13}C NMR (100 MHz, DMSO-d_6): δ 168.2, 161.6, 150.2, 142.5, 133.5, 131.7, 131.6, 128.9, 128.8, 127.9, 122.9, 122.6, 119.4, 96.5, 62.1, 52.8, 31.7, 29.0, 16.5. ESI-MS m/z: 560.3 $[M + H]^+$, 682.4 $[M + Na]^+$. $C_{33}H_{33}N_7O_2$ (559.27). HPLC purity: 97.44%.

*(E)-4-((4-((4-(4-(2-Cyanovinyl)-2,6-dimethylphenoxy)-5-(2-methoxypyridin-4-yl)pyrimidin-2-yl)amino)piperidin-1-yl)methyl)-benzenesulfonamide (**23a**).* **23a** was synthesized from **21a** (644 mg, 1.0 mmol) and (2-methoxypyridin-4-yl)boronic acid (183 mg, 1.2 mmol). White solid, 65% yield, mp: 132−134 °C. ^1H NMR (400 MHz, DMSO-d_6): δ 8.51 (d, J = 6.1 Hz, 1H), 8.19 (d, J = 5.4 Hz, 1H), 7.78 (d, J = 7.7 Hz, 2H), 7.59 (d, J = 15.4 Hz, 1H, ArCH═), 7.46−7.42 (m, 5H), 7.37−7.30 (m, 3H), 7.14 (s, 1H, NH), 6.50−6.34 (m, 1H, ═CHCN), 3.88 (s, 3H, OCH_3), 3.44 (s, 2H, N−CH_2), 2.77−2.74 (m, 2H), 2.06 (s, 6H), 1.99−1.17 (m, 7H). ^{13}C NMR (100 MHz, DMSO-d_6): δ 168.7, 164.5, 161.5, 155.2, 150.7, 147.3, 147.3, 143.4, 143.1, 131.6, 129.4, 128.6, 128.2, 126.0, 119.4, 116.9, 116.5, 109.1, 108.7, 96.4, 62.0, 53.5, 52.6, 31.2, 16.5. ESI-MS m/z: 626.4 $[M + H]^+$, 643.7 $[M + NH_4]^+$. $C_{33}H_{35}N_7O_4S$ (625.25). HPLC purity: 98.55%.

*(E)-3-(4-((5-(2-Methoxypyridin-4-yl)-2-((1-(4-(methylsulfonyl)-benzyl)piperidin-4-yl)amino)pyrimidin-4-yl)oxy)-3,5-dimethylphenyl)acrylonitrile (**23b**).* **23b** was synthesized from **21b** (643 mg, 1.0 mmol) and (2-methoxypyridin-4-yl)boronic acid (183 mg, 1.2 mmol). White solid, 65% yield, mp: 225−227 °C. ^1H NMR (400 MHz, DMSO-d_6): δ 8.51 (d, J = 6.1 Hz, 1H), 8.24−8.11 (m, 1H), 7.88 (d, J = 7.8 Hz, 2H), 7.68−7.49 (m, 4H), 7.45 (d, J = 5.2 Hz, 2H), 7.36−7.29 (m, 1H), 7.13 (s, 1H, NH), 6.40 (d, J = 16.7 Hz, 1H, ═CHCN), 3.87 (s, 3H, OCH_3), 3.54 (s, 2H, N−CH_2), 3.20 (s, 3H, SO_2CH_3), 2.75−2.60 (m, 2H), 2.05 (s, 6H), 1.96−1.12 (m, 7H). ^{13}C NMR (100 MHz, DMSO-d_6): δ 168.7, 164.4, 161.6, 147.3, 145.5, 139.8, 137.4, 131.5, 129.7, 127.4, 119.4, 116.5, 108.7, 96.4, 61.9, 53.5, 52.6, 44.0, 31.7, 29.0, 16.7. ESI-MS m/z: 625.3 $[M + H]^+$. $C_{34}H_{36}N_6O_4S$ (624.25). HPLC purity: 97.90%.

*(E)-4-((4-((4-(4-(2-Cyanovinyl)-2,6-dimethylphenoxy)-5-(2-methoxypyridin-4-yl)pyrimidin-2-yl)amino)piperidin-1-yl)methyl)-benzamide (**23c**).* **23c** was synthesized from **21c** (608 mg, 1.0 mmol) and (2-methoxypyridin-4-yl)boronic acid (183 mg, 1.2 mmol). White solid, 72% yield, mp: 170−172 °C. ^1H NMR (400 MHz, DMSO-d_6): δ 8.51−8.37 (m, 2H), 7.80 (d, J = 7.8 Hz, 2H), 7.59 (d, J = 16.4 Hz, 1H, ArCH═), 7.45−7.42 (m, 3H), 7.40−7.39 (m, 2H), 7.37−7.30 (m, 3H), 7.14 (s, 1H, NH), 6.44 (d, J = 16.7 Hz, 1H, ═CHCN), 3.87 (s, 3H, OCH_3), 3.43 (s, 2H, N−CH_2), 2.73−2.71 (m, 2H), 2.04 (s, 6H), 1.99−1.21 (m, 7H). ^{13}C NMR (100 MHz, DMSO-d_6): δ 168.7, 154.5, 161.7, 155.2, 150.7, 147.5, 147.3, 143.4, 142.8, 131.6, 129.4, 128.6, 128.0, 126.5, 119.4, 116.8, 109.1, 108.7, 96.4, 62.2, 53.5, 52.6, 31.5, 16.7. ESI-MS m/z: 590.2 $[M + H]^+$, 612.4 $[M + Na]^+$. $C_{34}H_{35}N_7O_3$ (589.28). HPLC purity: 98.11%.

(E)-4-((4-((4-(4-(2-Cyanovinyl)-2,6-dimethylphenoxy)-5-(2-methylpyridin-4-yl)pyrimidin-2-yl)amino)piperidin-1-yl)methyl)-

https://doi.org/10.1021/acs.jmedchem.1c00268
J. Med. Chem. 2021, 64, 4239−4256

*benzenesulfonamide (**24a**).* **24a** was synthesized from **21a** (644 mg, 1.0 mmol) and (2-methylpyridin-4-yl)boronic acid (164 mg, 1.2 mmol). White solid, 57% yield, mp: 138−140 °C. ^{1}H NMR (400 MHz, DMSO-d_6): δ 8.40 (dd, J = 13.9, 7.8 Hz, 2H), 7.71 (d, J = 7.7 Hz, 2H), 7.58−7.40 (m, 3H), 7.38 (d, J = 6.5 Hz, 4H), 7.24 (d, J = 5.2 Hz, 2H), 6.88 (s, 1H, NH), 6.34 (d, J = 17.3 Hz, 1H, =CHCN), 3.43 (s, 2H, N−CH_2), 3.20 (s, 3H, CH_3), 2.68 (d, J = 12.1 Hz, 2H), 1.99 (s, 6H), 1.84−1.17 (m, 7H). ^{13}C NMR (100 MHz, DMSO-d_6): δ 167.9, 165.2, 161.5, 160.3, 158.5, 152.1, 150.6, 150.4, 149.5, 143.4, 143.1, 142.0, 131.7, 129.4, 128.6, 128.2, 126.0, 122.1, 120.0, 119.4, 107.1, 96.4, 62.0, 52.5, 48.6, 31.7, 24.7, 16.5. ESI-MS m/z: 610.7 [M + H]$^+$, 632.4 [M + Na]$^+$. $C_{33}H_{35}N_7O_3S$ (609.25). HPLC purity: 99.05%.

*(E)-3-(3,5-Dimethyl-4-((5-(2-methylpyridin-4-yl)-2-((1-(4-(methylsulfonyl)benzyl)piperidin-4-yl)amino)pyrimidin-4-yl)oxy)-phenyl)acrylonitrile (**24b**).* **24b** was synthesized from **21b** (643 mg, 1.0 mmol) and (2-methylpyridin-4-yl)boronic acid (164 mg, 1.2 mmol). White solid, 58% yield, mp: 125−127 °C. ^{1}H NMR (400 MHz, DMSO-d_6): δ 8.47 (dd, J = 14.3, 7.6 Hz, 2H), 7.88 (d, J = 7.8 Hz, 2H), 7.57 (dt, J = 25.1, 13.8 Hz, 5H), 7.46 (s, 2H), 6.89 (s, 1H, NH), 6.41 (d, J = 16.7 Hz, 1H, =CHCN), 3.54−3.42 (m, 2H, N−CH_2), 3.20 (s, 3H, SO_2CH_3), 2.84−3.76 (m, 2H), 2.48 (s, 3H, CH_3), 2.06 (s, 6H), 2.00−1.19 (m, 7H). ^{13}C NMR (100 MHz, DMSO-d_6): δ 170.7, 167.2, 165.3, 161.5, 158.5, 150.8, 149.5, 145.5, 139.8, 131.5, 129.8, 127.4, 120.4, 105.9, 96.7, 61.9, 52.8, 44.0, 31.2, 24.7, 16.8. ESI-MS m/z: 609.7 [M + H]$^+$, 626.5 [M + NH_4]$^+$. $C_{34}H_{36}N_6O_3S$ (608.26). HPLC purity: 99.36%.

*(E)-4-((4-((4-(4-(2-Cyanovinyl)-2,6-dimethylphenoxy)-5-(2-methylpyridin-4-yl)pyrimidin-2-yl)amino)piperidin-1-yl)methyl)-benzamide (**24c**).* **24c** was synthesized from **21c** (608 mg, 1.0 mmol) and (2-methylpyridin-4-yl)boronic acid (164 mg, 1.2 mmol). White solid, 61% yield, mp: 127−129 °C. ^{1}H NMR (400 MHz, DMSO-d_6): δ 8.40 (dd, J = 13.8, 7.4 Hz, 2H), 7.84 (s, 1H), 7.75 (d, J = 7.7 Hz, 2H), 7.50−7.44 (m, 3H), 7.39 (s, 2H), 7.32−7.14 (m, 3H), 6.89 (s, 1H, NH), 6.42−6.27 (m, 1H, =CHCN), 3.40 (s, 2H, N−CH_2), 3.20 (s, 3H, CH_3), 2.72 (d, J = 26.0 Hz, 2H), 1.96 (s, 6H), 1.91−1.12 (m, 7H). ^{13}C NMR (100 MHz, DMSO-d_6): δ 168.2, 165.3, 158.4, 150.5, 149.5, 142.5, 133.4, 131.6, 128.8, 127.8, 121.6, 119.4, 114.4, 96.6, 62.3, 57.6, 52.8, 31.7, 24.7, 16.8. ESI-MS m/z: 574.5 [M + H]$^+$, 596.3 [M + Na]$^+$. $C_{34}H_{35}N_7O_2$ (573.29). HPLC purity: 98.77%.

*(E)-4-((4-((4-(4-(2-Cyanovinyl)-2,6-dimethylphenoxy)-5-(2-fluoropyridin-4-yl)pyrimidin-2-yl)amino)piperidin-1-yl)methyl)-benzenesulfonamide (**25a**).* **25a** was synthesized from **21a** (644 mg, 1.0 mmol) and (2-fluoropyridin-4-yl)boronic acid (169 mg, 1.2 mmol). White solid, 59% yield, mp: 222−224 °C. ^{1}H NMR (400 MHz, DMSO-d_6): δ 8.56 (d, J = 12.0 Hz, 1H), 8.19 (d, J = 5.3 Hz, 1H), 7.71−7.62 (m, 5H), 7.50−7.37 (m, 4H), 7.25 (d, J = 10.6 Hz, 2H), 6.89 (s, 1H, NH), 6.36 (d, J = 15.6 Hz, 1H, =CHCN), 3.58−3.28 (m, 2H, N−CH_2), 2.69 (s, 2H), 2.00 (s, 6H), 1.90−1.20 (m, 7H). ^{13}C NMR (100 MHz, DMSO-d_6): δ 165.1, 160.7, 156.0, 153.1, 151.9, 150.6, 150.4, 148.1, 143.4, 131.7 (d, J_{CF} = 13 Hz), 129.3, 128.6, 128.2 (d, J_{CF} = 8 Hz), 126.1, 121.3, 119.3, 104.6, 96.9, 52.5, 45.8, 29.0, 16.8. ESI-MS m/z: 614.4 [M + H]$^+$, 636.5 [M + Na]$^+$. $C_{32}H_{32}FN_7O_3S$ (613.23). HPLC purity: 98.95%.

*(E)-3-(4-((5-(2-Fluoropyridin-4-yl)-2-((1-(4-(methylsulfonyl)-benzyl)piperidin-4-yl)amino)pyrimidin-4-yl)oxy)-3,5-dimethylphenyl)acrylonitrile (**25b**).* **25b** was synthesized from **21b** (643 mg, 1.0 mmol) and (2-fluoropyridin-4-yl)boronic acid (169 mg, 1.2 mmol). White solid, 57% yield, mp: 147−149 °C. ^{1}H NMR (400 MHz, DMSO-d_6): δ 8.63 (d, J = 11.2 Hz, 1H), 8.31−8.22 (m, 1H), 7.88 (d, J = 7.9 Hz, 2H), 7.81−7.60 (m, 2H), 7.60−7.50 (m, 3H), 7.46 (d, J = 10.6 Hz, 2H), 6.70 (s, 1H, NH), 6.53−6.35 (m, 1H, =CHCN), 3.49−3.48 (m, 2H), 3.21 (s, 3H, SO_2CH_3), 2.94−2.55 (m, 2H), 2.07 (s, 6H), 1.95−1.05 (m, 7H). ^{13}C NMR (100 MHz, DMSO-d_6): δ 165.3, 160.7, 147.9, 145.4, 139.8, 132.5, 132.0 (d, J_{CF} = 10 Hz), 131.7, 131.6, 129.8 (d, J_{CF} = 9 Hz), 129.2 (d, J_{CF} = 11 Hz), 128.6, 128.2, 127.3, 120.8, 119.3, 107.4, 90.5, 52.7, 44.0, 31.7, 16.8. ESI-MS m/z: 613.4 [M + H]$^+$, 635.3 [M + Na]$^+$. $C_{33}H_{33}FN_6O_3S$ (612.23). HPLC purity: 98.56%.

*(E)-4-((4-((4-(4-(2-Cyanovinyl)-2,6-dimethylphenoxy)-5-(2-fluoropyridin-4-yl)pyrimidin-2-yl)amino)piperidin-1-yl)methyl)-benzamide (**25c**).* **25c** was synthesized from **21c** (608 mg, 1.0 mmol) and (2-fluoropyridin-4-yl)boronic acid (169 mg, 1.2 mmol). White solid, 49% yield, mp: 173−175 °C. ^{1}H NMR (400 MHz, DMSO-d_6): δ 8.63 (d, J = 11.1 Hz, 1H), 8.26 (d, J = 5.3 Hz, 1H), 8.04−7.54 (m, 5H), 7.46 (d, J = 10.6 Hz, 4H), 7.33 (d, J = 8.1 Hz, 2H), 6.70 (s, 1H, NH), 6.43 (d, J = 16.9 Hz, 1H, =CHCN), 3.41 (s, 2H, N−CH_2), 2.74 (s, 2H), 2.07 (s, 6H), 1.99−1.28 (m, 7H). ^{13}C NMR (100 MHz, DMSO-d_6): δ 168.2, 165.3, 158.8, 157.6, 152.7, 150.5, 148.1, 142.6, 133.2, 131.6, 127.9, 119.3, 115.0, 110.7, 107.0, 96.8, 52.5, 48.9, 29.0, 18.9, 16.5. ESI-MS m/z: 578.5 [M + H]$^+$, 600.5 [M + Na]$^+$. $C_{33}H_{32}FN_7O_2$ (577.26). HPLC purity: 97.77%.

*(E)-4-((4-((5-(2-Chloropyridin-4-yl)-4-(4-(2-cyanovinyl)-2,6-dimethylphenoxy)pyrimidin-2-yl)amino)piperidin-1-yl)methyl)-benzenesulfonamide (**26a**).* **26a** was synthesized from **21a** (644 mg, 1.0 mmol) and (2-chloropyridin-4-yl)boronic acid (188 mg, 1.2 mmol). White solid, 68% yield, mp: 133−135 °C. ^{1}H NMR (400 MHz, DMSO-d_6): δ 8.53 (d, J = 14.2 Hz, 1H), 8.35 (d, J = 5.2 Hz, 1H), 7.75−7.70 (m, 4H), 7.55 (d, J = 16.7 Hz, 1H, ArCH=), 7.38 (d, J = 10.7 Hz, 4H), 7.24 (d, J = 6.8 Hz, 2H), 6.90 (s, 1H, NH), 6.35 (d, J = 16.6 Hz, 1H, =CHCN), 3.43 (s, 2H, N−CH_2), 2.86−2.58 (m, 2H), 1.99 (s, 6H), 1.90−0.98 (m, 7H). ^{13}C NMR (100 MHz, DMSO-d_6): δ 168.4, 150.6, 145.7, 143.3, 143.1, 131.7, 129.4, 128.6, 128.2, 126.0, 122.0, 119.4, 105.7, 96.8, 62.0, 52.5, 49.7, 31.2, 23.8, 16.5. ESI-MS m/z: 630.7 [M + H]$^+$, 652.2 [M + Na]$^+$. $C_{32}H_{32}ClN_7O_3S$ (629.20). HPLC purity: 98.11%.

*(E)-3-(4-((5-(2-Chloropyridin-4-yl)-2-((1-(4-(methylsulfonyl)-benzyl)piperidin-4-yl)amino)pyrimidin-4-yl)oxy)-3,5-dimethylphenyl)acrylonitrile (**26b**).* **26b** was synthesized from **21b** (643 mg, 1.0 mmol) and (2-chloropyridin-4-yl)boronic acid (188 mg, 1.2 mmol). White solid, 51% yield, mp: 130−132 °C. ^{1}H NMR (400 MHz, DMSO-d_6): δ 8.60 (d, J = 14.0 Hz, 1H), 8.42 (d, J = 5.2 Hz, 1H), 7.87−7.81 (m, 3H), 7.76 (d, J = 8.9 Hz, 2H), 7.67−7.49 (m, 2H), 7.45 (d, J = 8.9 Hz, 2H), 6.89 (s, 1H, NH), 6.50−6.32 (m, 1H, =CHCN), 3.48 (s, 2H, N−CH_2), 3.20 (s, 3H, SO_2CH_3), 2.84−2.56 (m, 2H), 2.06 (s, 6H), 1.98−1.17 (m, 7H). ^{13}C NMR (100 MHz, DMSO-d_6): δ 168.7, 165.3, 161.8, 160.4, 153.6, 151.2, 150.6, 150.3, 145.5, 139.8, 131.7, 129.8, 128.6, 128.2, 127.4, 122.3, 119.4, 112.6, 96.5, 61.9, 52.6, 44.0, 31.7, 29.0, 16.6. ESI-MS m/z: 629.6 [M + H]$^+$, 646.2 [M + NH_4]$^+$. $C_{33}H_{33}ClN_6O_3S$ (628.20). HPLC purity: 97.28%.

*(E)-4-((4-((5-(2-Chloropyridin-4-yl)-4-(4-(2-cyanovinyl)-2,6-dimethylphenoxy)pyrimidin-2-yl)amino)piperidin-1-yl)methyl)-benzamide (**26c**).* **26c** was synthesized from **21c** (608 mg, 1.0 mmol) and (2-chloropyridin-4-yl)boronic acid (188 mg, 1.2 mmol). White solid, 57% yield, mp: 123−127 °C. ^{1}H NMR (400 MHz, DMSO-d_6): δ 8.53 (d, J = 13.4 Hz, 1H), 8.35 (d, J = 5.2 Hz, 1H), 7.84 (s, 1H), 7.75 (d, J = 7.9 Hz, 3H), 7.68 (d, J = 9.8 Hz, 1H), 7.54 (t, J = 17.3 Hz, 1H, ArCH=), 7.39 (s, 2H), 7.25 (dd, J = 14.0, 7.3 Hz, 3H), 6.89 (s, 1H, NH), 6.35 (d, J = 16.7 Hz, 1H, =CHCN), 3.40 (s, 2H, N−CH_2), 2.87−2.63 (m, 2H), 1.99 (s, 6H), 1.93−1.12 (m, 7H). ^{13}C NMR (100 MHz, DMSO-d_6): δ 168.2, 164.3, 161.7, 160.7, 152.4, 150.3, 145.5, 142.5, 133.4, 131.7, 128.9, 127.9, 122.4, 121.8, 119.3, 96.8, 62.3, 52.5, 31.2, 23.7, 16.5. ESI-MS m/z: 594.3 [M + H]$^+$, 616.5 [M + Na]$^+$. $C_{33}H_{32}ClN_7O_2$ (593.23). HPLC purity: 99.15%.

*(E)-4-((4-((5-(2-Bromopyridin-4-yl)-4-(4-(2-cyanovinyl)-2,6-dimethylphenoxy)pyrimidin-2-yl)amino)piperidin-1-yl)methyl)-benzenesulfonamide (**27a**).* **27a** was synthesized from **21a** (644 mg, 1.0 mmol) and (2-bromopyridin-4-yl)boronic acid (241 mg, 1.2 mmol). White solid, 64% yield, mp: 183−185 °C. ^{1}H NMR (400 MHz, DMSO-d_6): δ 8.56 (d, J = 11.4 Hz, 1H), 8.20 (d, J = 5.3 Hz, 1H), 7.71−7.62 (m, 3H), 7.57−7.55 (m, 2H), 7.50−7.37 (m, 4H), 7.25 (d, J = 8.6 Hz, 2H), 6.89 (s, 1H, NH), 6.36−6.35 (m, 1H, =CHCN), 3.58−3.28 (m, 2H, N−CH_2), 2.69 (s, 2H), 2.00 (s, 6H), 1.90−1.20 (m, 7H). ^{13}C NMR (100 MHz, DMSO-d_6): δ 170.2, 165.8, 161.5, 156.9, 153.9, 151.3, 144.5, 143.4, 137.7, 131.7, 129.4, 126.9, 126.2, 122.2, 107.9, 90.7, 52.6, 50.6, 45.8, 29.0, 16.5. ESI-MS m/z: 674.5 [M + H]$^+$, 696.4 [M + Na]$^+$. $C_{32}H_{32}BrN_7O_3S$ (673.15). HPLC purity: 98.66%.

*(E)-3-(4-((5-(2-Bromopyridin-4-yl)-2-((1-(4-(methylsulfonyl)-benzyl)piperidin-4-yl)amino)pyrimidin-4-yl)oxy)-3,5-dimethylphenyl)acrylonitrile (**27b**).* **27b** was synthesized from **21b** (643 mg, 1.0 mmol) and (2-bromopyridin-4-yl)boronic acid (241 mg,

https://doi.org/10.1021/acs.jmedchem.1c00268
J. Med. Chem. 2021, 64, 4239−4256

1.2 mmol). White solid, 57% yield, mp: 157−159 °C. ^{1}H NMR (400 MHz, DMSO-d_6): δ 8.41 (s, 1H), 7.87 (d, J = 7.1 Hz, 2H), 7.65−7.49 (m, 4H), 7.45 (s, 2H), 7.28−7.14 (m, 2H), 6.70 (s, 1H, NH), 6.40 (d, J = 16.7 Hz, 1H, =CHCN), 3.56−3.52 (m, 2H), 3.19 (s, 3H, SO_2CH_3), 2.74 (s, 2H), 2.05 (s, 6H), 1.98−1.39 (m, 7H). ^{13}C NMR (100 MHz, DMSO-d_6): δ 166.2, 161.4, 150.5, 145.4, 145.4, 139.8, 131.7, 131.6, 131.4, 131.1, 129.8, 129.7, 128.6, 127.3, 120.7, 119.3, 101.2, 96.2, 61.9, 52.7, 50.6, 29.0, 16.5. ESI-MS m/z: 673.5 $[M + H]^+$, 695.2 $[M + Na]^+$. $C_{33}H_{33}BrN_6O_3S$ (672.15). HPLC purity: 99.54%.

*(E)-4-((4-((5-(2-Bromopyridin-4-yl)-4-(4-(2-cyanovinyl)-2,6-dimethylphenoxy)pyrimidin-2-yl)amino)piperidin-1-yl)methyl)-benzamide (**27c**).* **27c** was synthesized from **21c** (608 mg, 1.0 mmol) and (2-bromopyridin-4-yl)boronic acid (241 mg, 1.2 mmol). White solid, 55% yield, mp: 178−180 °C. ^{1}H NMR (400 MHz, DMSO-d_6): δ 8.41−8.40 (m, 1H), 7.95 (s, 2H), 7.83 (d, J = 7.1 Hz, 2H), 7.69−7.54 (m, 3H), 7.46 (s, 2H), 7.30−7.28 (m, 3H), 6.71 (s, 1H, NH), 6.43 (d, J = 16.7 Hz, 1H, =CHCN), 3.42 (s, 2H, N−CH_2), 2.75 (s, 2H), 2.10 (s, 6H), 1.97−1.12 (m, 7H). ^{13}C NMR (100 MHz, DMSO-d_6): δ 168.2, 165.8, 161.3, 157.1, 151.4, 150.5, 146.1, 144.2, 142.6, 133.7, 131.7, 131.4, 131.0, 128.9, 127.9, 122.9, 119.3, 110.0, 100.4, 96.5, 52.7, 50.6, 29.0, 16.4. ESI-MS m/z: 638.4 $[M + H]^+$, 655.4 $[M + NH_4]^+$. $C_{33}H_{32}BrN_7O_2$ (637.18). HPLC purity: 99.18%.

*(E)-4-((4-((4-(4-(2-Cyanovinyl)-2,6-dimethylphenoxy)-5-(pyridin-3-yl)pyrimidin-2-yl)amino)piperidin-1-yl)methyl)-benzenesulfonamide (**28a**).* **28a** was synthesized from **21a** (644 mg, 1.0 mmol) and pyridin-3-ylboronic acid (147 mg, 1.2 mmol). White solid, 62% yield, mp: 148−150 °C. ^{1}H NMR (400 MHz, DMSO-d_6): δ 8.78 (d, J = 18.1 Hz, 1H), 8.45 (dd, J = 4.8, 1.6 Hz, 1H), 8.34 (d, J = 3.3 Hz, 1H), 7.98 (s, 1H), 7.71 (d, J = 7.9 Hz, 2H), 7.51−7.39 (m, 6H), 7.31−7.21 (m, 2H), 7.11 (d, J = 8.2 Hz, 1H), 6.34 (d, J = 17.5 Hz, 1H, =CHCN), 3.42 (s, 2H), 2.88−2.52 (m, 2H), 1.99 (s, 6H), 1.82−1.12 (m, 7H). ^{13}C NMR (100 MHz, DMSO): δ 165.2, 161.4, 160.0, 159.5, 149.2, 148.2, 143.4, 143.1, 136.2, 131.6, 129.4, 128.1, 126.0, 124.0, 119.4, 113.7, 96.6, 91.2, 61.9, 52.8, 31.2, 29.0, 16.6. ESI-MS m/z: 596.3 $[M + H]^+$, 618.5 $[M + Na]^+$. $C_{32}H_{33}N_7O_3S$ (595.24). HPLC purity: 98.99%.

*(E)-3-(3,5-Dimethyl-4-((2-((1-(4-(methylsulfonyl)benzyl)-piperidin-4-yl)amino)-5-(pyridin-3-yl)pyrimidin-4-yl)oxy)phenyl)-acrylonitrile (**28b**).* **28b** was synthesized from **21b** (643 mg, 1.0 mmol) and pyridin-3-ylboronic acid (147 mg, 1.2 mmol). White solid, 39% yield, mp: 193−195 °C. ^{1}H NMR (400 MHz, DMSO-d_6): δ 8.78 (d, J = 17.4 Hz, 1H), 8.45 (dd, J = 4.7, 1.6 Hz, 1H), 8.34 (d, J = 3.3 Hz, 1H), 7.99 (d, J = 13.9 Hz, 1H), 7.81 (d, J = 7.9 Hz, 2H), 7.59−7.35 (m, 7H), 6.34 (d, J = 16.7 Hz, 1H, =CHCN), 3.41 (s, 2H), 3.14 (s, 3H, SO_2CH_3), 2.84−2.49 (m, 2H), 1.99 (s, 6H), 1.78−1.12 (m, 7H). ^{13}C NMR (100 MHz, DMSO): δ 165.2, 161.4, 159.6, 154.7, 152.1, 150.6, 149.3, 148.2, 145.5, 139.8, 136.1, 135.8, 131.6, 131.5, 129.7, 127.4, 124.0, 119.4, 106.5, 96.7, 61.9, 52.6, 44.0, 31.3, 16.6. ESI-MS m/z: 595.5 $[M + H]^+$, 617.4 $[M + Na]^+$. $C_{33}H_{34}N_6O_3S$ (594.24). HPLC purity: 98.41%.

*(E)-4-((4-((4-(4-(2-Cyanovinyl)-2,6-dimethylphenoxy)-5-(pyridin-3-yl)pyrimidin-2-yl)amino)piperidin-1-yl)methyl)benzamide (**28c**).* **28c** was synthesized from **21c** (608 mg, 1.0 mmol) and pyridin-3-ylboronic acid (147 mg, 1.2 mmol). White solid, 37% yield, mp: 234−236 °C. ^{1}H NMR (400 MHz, DMSO-d_6): δ 8.78 (d, J = 17.3 Hz, 1H), 8.50−8.41 (m, 1H), 8.34 (d, J = 3.0 Hz, 1H), 7.99 (d, J = 12.6 Hz, 1H), 7.86 (s, 1H), 7.76 (d, J = 7.8 Hz, 2H), 7.55 (d, J = 17.7 Hz, 1H), 7.46−7.35 (m, 3H), 7.29−7.25 (m, 3H), 7.10 (d, J = 7.1 Hz, 1H), 6.34 (d, J = 16.7 Hz, 1H, =CHCN), 3.41 (s, 2H), 2.84−2.60 (m, 2H), 1.99 (s, 6H), 1.87−1.12 (m, 7H). ^{13}C NMR (100 MHz, DMSO-d_6): δ 168.2, 165.2, 161.4, 159.5, 150.5, 149.1, 148.2, 136.2, 133.4, 131.6, 131.5, 128.8, 127.8, 124.0, 119.4, 96.6, 90.7, 62.2, 52.7, 39.6, 16.7. ESI-MS m/z: 560.2 $[M + H]^+$, 577.5 $[M + NH_4]^+$. $C_{33}H_{33}N_7O_2$ (559.27). HPLC purity: 97.55%.

*(E)-4-((4-((5-(6-Aminopyridin-3-yl)-4-(4-(2-cyanovinyl)-2,6-dimethylphenoxy)pyrimidin-2-yl)amino)piperidin-1-yl)methyl)-benzenesulfonamide (**29a**).* **29a** was synthesized from **21a** (644 mg, 1.0 mmol) and (6-aminopyridin-3-yl)boronic acid (165 mg, 1.2 mmol). White solid, 51% yield, mp: 146−148 °C. ^{1}H NMR (400 MHz, DMSO-d_6): δ 8.16 (d, J = 3.4 Hz, 1H), 8.06 (s, 1H), 7.71 (dd, J = 8.3, 2.7 Hz, 2H), 7.56−7.52 (m, 3H), 7.38 (d, J = 6.5 Hz, 4H), 7.25 (s, 2H), 6.45 (d, J = 8.6 Hz, 1H), 6.33 (d, J = 16.7 Hz, 1H, =CHCN), 5.93 (s, 2H), 3.40 (s, 2H, N−CH_2), 2.87−2.74 (m, 2H), 1.97 (s, 6H), 1.82−1.02 (m, 7H). ^{13}C NMR (100 MHz, DMSO-d_6): δ 165.2, 160.7, 159.1, 152.4, 150.6, 147.3, 143.1, 137.6, 131.6, 131.3, 129.4, 128.4, 126.0, 119.4, 118.1, 108.0, 96.4, 62.0, 52.7, 31.5, 16.7. ESI-MS m/z: 611.3 $[M + H]^+$, 633.7 $[M + Na]^+$. $C_{32}H_{34}N_8O_3S$ (610.25). HPLC purity: 98.63%.

*(E)-3-(4-((5-(6-Aminopyridin-3-yl)-2-((1-(4-(methylsulfonyl)-benzyl)piperidin-4-yl)amino)pyrimidin-4-yl)oxy)-3,5-dimethylphenyl)acrylonitrile (**29b**).* **29b** was synthesized from **21b** (643 mg, 1.0 mmol) and (6-aminopyridin-3-yl)boronic acid (165 mg, 1.2 mmol). White solid, 40% yield, mp: 209−211 °C. ^{1}H NMR (400 MHz, DMSO-d_6): δ 8.23 (d, J = 3.4 Hz, 1H), 8.14 (s, 1H), 7.88 (d, J = 7.9 Hz, 2H), 7.62−7.57 (m, 3H), 7.53 (d, J = 7.7 Hz, 2H), 7.44 (s, 2H), 6.52 (d, J = 8.6 Hz, 1H), 6.40 (d, J = 16.7 Hz, 1H, =CHCN), 6.00 (s, 2H), 3.41 (s, 2H, N−CH_2), 3.20 (s, 3H, SO_2CH_3), 2.80−2.67 (m, 2H), 2.06 (s, 6H), 1.87−1.21 (m, 7H). ^{13}C NMR (100 MHz, DMSO-d_6): δ 165.2, 160.7, 159.1, 148.6, 147.3, 145.5, 139.8, 137.6, 131.6, 131.3, 129.8, 129.7, 127.4, 119.4, 118.1, 108.0, 61.9, 52.7, 44.0, 31.6, 16.7. ESI-MS m/z: 611.2 $[M + H]^+$. $C_{33}H_{35}N_7O_3S$ (609.25). HPLC purity: 98.39%.

*(E)-4-((4-((5-(6-Aminopyridin-3-yl)-4-(4-(2-cyanovinyl)-2,6-dimethylphenoxy)pyrimidin-2-yl)amino)piperidin-1-yl)methyl)-benzamide (**29c**).* **29c** was synthesized from **21c** (608 mg, 1.0 mmol) and (6-aminopyridin-3-yl)boronic acid (165 mg, 1.2 mmol). White solid, 47% yield, mp: 182−184 °C. ^{1}H NMR (400 MHz, DMSO-d_6): δ 8.23 (d, J = 3.8 Hz, 1H), 8.13 (s, 1H), 7.96 (s, 1H), 7.84 (d, J = 7.8 Hz, 2H), 7.61 (d, J = 14.4 Hz, 3H), 7.44 (s, 2H), 7.40−7.27 (m, 4H), 6.53 (d, J = 8.6 Hz, 1H), 6.41 (d, J = 16.7 Hz, 1H, =CHCN), 6.02 (s, 2H), 3.41 (s, 2H, N−CH_2), 2.81−2.58 (m, 2H), 2.05 (s, 6H), 1.82−1.10 (m, 7H). ^{13}C NMR (100 MHz, DMSO): δ 172.4, 168.2, 165.1, 160.7, 159.1, 150.5, 147.3, 144.4, 137.7, 131.6, 130.1, 129.3, 127.9, 119.4, 118.0, 108.0, 96.5, 90.0, 53.8, 33.1, 29.5, 16.7. ESI-MS m/z: 575.3 $[M + H]^+$, 597.1 $[M + Na]^+$. $C_{33}H_{34}N_8O_2$ (574.28). HPLC purity: 98.06%.

*(E)-4-((4-((4-(4-(2-Cyanovinyl)-2,6-dimethylphenoxy)-5-(6-fluoropyridin-3-yl)pyrimidin-2-yl)amino)piperidin-1-yl)methyl)-benzenesulfonamide (**30a**).* **30a** was synthesized from **21a** (644 mg, 1.0 mmol) and (6-fluoropyridin-3-yl)boronic acid (169 mg, 1.2 mmol). White solid, 71% yield, mp: 118−120 °C. ^{1}H NMR (400 MHz, DMSO-d_6): δ 8.41 (d, J = 18.3 Hz, 1H), 8.33 (s, 1H), 8.18 (s, 1H), 7.71 (dd, J = 7.1, 3.6 Hz, 2H), 7.62−7.48 (m, 1H), 7.39 (d, J = 11.2 Hz, 4H), 7.28−7.17 (m, 4H), 6.34 (d, J = 16.5 Hz, 1H, =CHCN), 3.55−3.52 (m, 2H), 2.81−2.50 (m, 2H), 1.99 (s, 6H), 1.75−1.15 (m, 7H). ^{13}C NMR (100 MHz, DMSO): δ 165.1, 161.5, 159.5, 152.5, 150.6, 148.5, 146.9 (J_{CF} = 20 Hz), 143.4 (J_{CF} = 23 Hz), 142.1, 131.6, 131.5, 128.7, 126.9, 126.0, 119.4, 110.0, 109.6, 104.4, 96.6, 62.0, 52.8, 31.7, 29.0, 16.8. ESI-MS m/z: 614.2 $[M + H]^+$, 636.4 $[M + Na]^+$. $C_{32}H_{32}FN_7O_3S$ (613.23). HPLC purity: 99.23%.

*(E)-3-(4-((5-(6-Fluoropyridin-3-yl)-2-((1-(4-(methylsulfonyl)-benzyl)piperidin-4-yl)amino)pyrimidin-4-yl)oxy)-3,5-dimethylphenyl)acrylonitrile (**30b**).* **30b** was synthesized from **21b** (643 mg, 1.0 mmol) and (6-fluoropyridin-3-yl)boronic acid (169 mg, 1.2 mmol). White solid, 61% yield, mp: 115−117 °C. ^{1}H NMR (400 MHz, DMSO-d_6): δ 8.42 (d, J = 17.7 Hz, 1H), 8.33 (s, 1H), 8.17 (d, J = 8.5 Hz, 1H), 7.81 (d, J = 8.0 Hz, 2H), 7.57−7.41 (m, 4H), 7.38 (s, 2H), 7.20 (dd, J = 8.6, 2.9 Hz, 1H), 6.34 (d, J = 16.7 Hz, 1H, =CHCN), 3.46−3.42 (m, 2H), 3.14 (s, 3H, SO_2CH_3), 2.79−2.49 (m, 2H), 1.99 (s, 6H), 1.76−1.06 (m, 7H). ^{13}C NMR (100 MHz, DMSO): δ 165.1, 161.5, 161.2, 160.0, 150.6, 146.9 (J_{CF} = 20 Hz), 145.5, 142.4, 139.8, 131.6 (J_{CF} = 10 Hz), 129.8, 128.7, 128.1, 127.4, 124.5, 119.4, 109.9, 96.6, 61.9, 52.6, 44.0, 31.7, 16.6. ESI-MS m/z: 613.5 $[M + H]^+$, 635.3 $[M + Na]^+$. $C_{33}H_{33}FN_6O_3S$ (612.23). HPLC purity: 97.95%.

*(E)-4-((4-((4-(4-(2-Cyanovinyl)-2,6-dimethylphenoxy)-5-(6-fluoropyridin-3-yl)pyrimidin-2-yl)amino)piperidin-1-yl)methyl)-benzamide (**30c**).* **30c** was synthesized from **21c** (608 mg, 1.0 mmol) and (6-fluoropyridin-3-yl)boronic acid (169 mg, 1.2 mmol). White solid, 65% yield, mp: 113−115 °C. ^{1}H NMR (400 MHz, DMSO-d_6): δ 8.41 (d, J = 17.7 Hz, 1H), 8.33 (s, 1H), 8.18 (s, 1H), 7.86 (s, 1H), 7.76 (d, J = 7.7 Hz, 2H), 7.60−7.47 (m, 1H), 7.38 (s, 2H), 7.31−7.09

https://doi.org/10.1021/acs.jmedchem.1c00268
J. Med. Chem. 2021, 64, 4239−4256

(m, 5H), 6.34 (d, J = 16.7 Hz, 1H, =CHCN), 3.54−3.53 (m, 2H), 2.77−2.73 (m, 2H), 1.99 (s, 6H), 1.83−1.10 (m, 7H). ^{13}C NMR (100 MHz, DMSO): δ 168.2, 165.1, 161.2, 159.4, 155.8, 150.4, 146.7, 142.4, 133.4, 131.6 (J_{CF} = 10 Hz), 128.8, 127.8, 119.4, 109.9, 109.6, 96.6, 62.3, 52.8, 31.5, 29.0, 16.8. ESI-MS m/z: 578.6 $[M + H]^+$, 600.4 $[M + Na]^+$. $C_{33}H_{32}FN_7O_2$ (577.26). HPLC purity: 98.52%.

■ ASSOCIATED CONTENT

Supporting Information

The Supporting Information is available free of charge at https://pubs.acs.org/doi/10.1021/acs.jmedchem.1c00268.

In vitro assay of anti-HIV activities in MT-4 cells, recombinant HIV-1 RT inhibitory assays, pharmacokinetic methods, acute toxicity experiment, and assay procedures for hERG activity (PDF)

■ AUTHOR INFORMATION

Corresponding Authors

Dongwei Kang − *Department of Medicinal Chemistry, Key Laboratory of Chemical Biology (Ministry of Education), School of Pharmaceutical Sciences, Cheeloo College of Medicine, Shandong University, Jinan 250012, Shandong, PR China; China-Belgium Collaborative Research Center for Innovative Antiviral Drugs of Shandong Province, Jinan 250012, Shandong, PR China;* orcid.org/0000-0001-9232-953X; Phone: 086-531-88382005; Email: kangdongwei@sdu.edu.cn

Eddy Arnold − *Center for Advanced Biotechnology and Medicine and Department of Chemistry and Chemical Biology, Rutgers University, Piscataway, New Jersey 08854, United States;* orcid.org/0000-0003-2612-9622; Phone: 848-445-9777; Email: arnold@cabm.rutgers.edu

Peng Zhan − *Department of Medicinal Chemistry, Key Laboratory of Chemical Biology (Ministry of Education), School of Pharmaceutical Sciences, Cheeloo College of Medicine, Shandong University, Jinan 250012, Shandong, PR China; China-Belgium Collaborative Research Center for Innovative Antiviral Drugs of Shandong Province, Jinan 250012, Shandong, PR China;* orcid.org/0000-0002-9675-6026; Phone: 086-531-88382005; Email: zhanpeng1982@sdu.edu.cn

Xinyong Liu − *Department of Medicinal Chemistry, Key Laboratory of Chemical Biology (Ministry of Education), School of Pharmaceutical Sciences, Cheeloo College of Medicine, Shandong University, Jinan 250012, Shandong, PR China; China-Belgium Collaborative Research Center for Innovative Antiviral Drugs of Shandong Province, Jinan 250012, Shandong, PR China;* orcid.org/0000-0002-7302-2214; Phone: 086-531-88380270; Email: xinyongl@sdu.edu.cn

Authors

Francesc X. Ruiz − *Center for Advanced Biotechnology and Medicine and Department of Chemistry and Chemical Biology, Rutgers University, Piscataway, New Jersey 08854, United States*

Yanying Sun − *Department of Medicinal Chemistry, Key Laboratory of Chemical Biology (Ministry of Education), School of Pharmaceutical Sciences, Cheeloo College of Medicine, Shandong University, Jinan 250012, Shandong, PR China*

Da Feng − *Department of Medicinal Chemistry, Key Laboratory of Chemical Biology (Ministry of Education), School of Pharmaceutical Sciences, Cheeloo College of Medicine, Shandong University, Jinan 250012, Shandong, PR China*

Lanlan Jing − *Department of Medicinal Chemistry, Key Laboratory of Chemical Biology (Ministry of Education), School of Pharmaceutical Sciences, Cheeloo College of Medicine, Shandong University, Jinan 250012, Shandong, PR China*

Zhao Wang − *Department of Medicinal Chemistry, Key Laboratory of Chemical Biology (Ministry of Education), School of Pharmaceutical Sciences, Cheeloo College of Medicine, Shandong University, Jinan 250012, Shandong, PR China*

Tao Zhang − *Department of Medicinal Chemistry, Key Laboratory of Chemical Biology (Ministry of Education), School of Pharmaceutical Sciences, Cheeloo College of Medicine, Shandong University, Jinan 250012, Shandong, PR China*

Shenghua Gao − *Department of Medicinal Chemistry, Key Laboratory of Chemical Biology (Ministry of Education), School of Pharmaceutical Sciences, Cheeloo College of Medicine, Shandong University, Jinan 250012, Shandong, PR China*

Lin Sun − *Department of Medicinal Chemistry, Key Laboratory of Chemical Biology (Ministry of Education), School of Pharmaceutical Sciences, Cheeloo College of Medicine, Shandong University, Jinan 250012, Shandong, PR China;* orcid.org/0000-0002-8395-5886

Erik De Clercq − *Rega Institute for Medical Research, Laboratory of Virology and Chemotherapy, Katholieke Universiteit Leuven, Leuven B-3000, Belgium;* orcid.org/0000-0002-2985-8890

Christophe Pannecouque − *Rega Institute for Medical Research, Laboratory of Virology and Chemotherapy, Katholieke Universiteit Leuven, Leuven B-3000, Belgium*

Complete contact information is available at: https://pubs.acs.org/10.1021/acs.jmedchem.1c00268

Notes

The authors declare no competing financial interest.

The authors declare that all experimental work complied with the institutional guidelines on animal studies (care and use of laboratory animals).

■ ACKNOWLEDGMENTS

We gratefully acknowledge financial support from the National Natural Science Foundation of China (NSFC nos. 81973181, 81903453), Shandong Provincial Key Research and Development Project (nos. 2019JZZY021011), Shandong Provincial Natural Science Foundation (ZR2019BH011, ZR2020YQ61, ZR2020JQ31), Foreign Cultural and Educational Experts Project (GXL20200015001), Young Scholars Program of Shandong University (YSPSDU no. 2016WLJH32), National Science and Technology Major Projects for "Major New Drugs Innovation and Development" (2019ZX09301126), the Taishan Scholar Program at Shandong Province, KU Leuven (GOA 10/014), and NIH grant R01 AI027690 (to E.A.). The technical assistance of Kris Uyttersprot and Kristien Erven for the HIV experiments is gratefully acknowledged.

ABBREVIATIONS

AIDS, acquired immune deficiency syndrome; cART, combination antiretroviral therapy; CC_{50}, 50% cytotoxicity concentration; C_{max}, maximum concentration; DAPY, diarylpyrimidine; DLV, delavirdine; DOR, doravirine; EFV, efavirenz; ETV, etravirine; EC_{50}, the effective concentration causing 50% inhibition of viral cytopathogenicity; FDA, U.S. Food and Drug Administration; HIV, human immunodeficiency virus; hERG, the human ether-à-go-go related gene; NNIBP, NNRTI-binding pocket; NNRTI, non-nucleoside RT inhibitor; NRTI, nucleoside RT inhibitor; NVP, nevirapine; RF, fold-resistance; RPV, rilpivirine; RT, reverse transcriptase; SAR, structure−activity relationship; SI, selectivity index; TLC, thin layer chromatography; TMS, tetramethylsilane; WT, wild type

REFERENCES

(1) https://www.who.int/hiv/data/en/ (accessed 2021-02-01).

(2) Bec, G.; Meyer, B.; Gerard, M.-A.; Steger, J.; Fauster, K.; Wolff, P.; Burnouf, D.; Micura, R.; Dumas, P.; Ennifar, E. Thermodynamics of HIV-1 reverse transcriptase in action elucidates the mechanism of action of non-nucleoside inhibitors. *J. Am. Chem. Soc.* **2013**, *135*, 9743−9752.

(3) Namasivayam, V.; Vanangamudi, M.; Kramer, V. G.; Kurup, S.; Zhan, P.; Liu, X.; Kongsted, J.; Byrareddy, S. N. The journey of HIV-1 non-nucleoside reverse transcriptase inhibitors (NNRTIs) from lab to clinic. *J. Med. Chem.* **2019**, *62*, 4851−4883.

(4) Zhuang, C.; Pannecouque, C.; De Clercq, E.; Chen, F. Development of non-nucleoside reverse transcriptase inhibitors (NNRTIs): our past twenty years. *Acta Pharm. Sin. B* **2020**, *10*, 961−978.

(5) Cilento, M. E.; Kirby, K. A.; Sarafianos, S. G. Avoiding drug resistance in hiv reverse transcriptase. *Chem. Rev.* **2021**, DOI: 10.1021/acs.chemrev.0c00967.

(6) Beyrer, C.; Pozniak, A. HIV drug resistance—an emerging threat to epidemic control. *N. Engl. J. Med.* **2017**, *377*, 1605−1607.

(7) Battini, L.; Bollini, M. Challenges and approaches in the discovery of human immunodeficiency virus type-1 non-nucleoside reverse transcriptase inhibitors. *Med. Res. Rev.* **2019**, *39*, 1235−1273.

(8) Kang, D.; Fang, Z.; Li, Z.; Huang, B.; Zhang, H.; Lu, X.; Xu, H.; Zhou, Z.; Ding, X.; Daelemans, D.; De Clercq, E.; Pannecouque, C.; Zhan, P.; Liu, X. Design, synthesis, and evaluation of thiophene[3,2-d]pyrimidine derivatives as HIV-1 non-nucleoside reverse transcriptase inhibitors with significantly improved drug resistance profiles. *J. Med. Chem.* **2016**, *59*, 7991−8007.

(9) Kang, D.; Fang, Z.; Huang, B.; Lu, X.; Zhang, H.; Xu, H.; Huo, Z.; Zhou, Z.; Yu, Z.; Meng, Q.; Wu, G.; Ding, X.; Tian, Y.; Daelemans, D.; De Clercq, E.; Pannecouque, C.; Zhan, P.; Liu, X. Structure-based optimization of thiophene[3,2-d]pyrimidine derivatives as potent HIV-1 non-nucleoside reverse transcriptase inhibitors with improved potency against resistance-associated variants. *J. Med. Chem.* **2017**, *60*, 4424−4443.

(10) Yang, Y.; Kang, D.; Nguyen, L. A.; Smithline, Z. B.; Pannecouque, C.; Zhan, P.; Liu, X.; Steitz, T. A. Structural basis for potent and broad inhibition of HIV-1 RT by thiophene[3,2-d] pyrimidine non-nucleoside inhibitors. *eLife* **2018**, *7*, No. e36340.

(11) Kang, D.; Zhang, H.; Wang, Z.; Zhao, T.; Ginex, T.; Luque, F. J.; Yang, Y.; Wu, G.; Feng, D.; Wei, F.; Zhang, J.; De Clercq, E.; Pannecouque, C.; Chen, C. H.; Lee, K.-H.; Murugan, N. A.; Steitz, T. A.; Zhan, P.; Liu, X. Identification of dihydrofuro[3,4-d]pyrimidine derivatives as novel HIV-1 non-nucleoside reverse transcriptase inhibitors with promising antiviral activities and desirable physicochemical properties. *J. Med. Chem.* **2019**, *62*, 1484−1501.

(12) Ishikawa, M.; Hashimoto, Y. Improvement in aqueous solubility in small molecule drug discovery programs by disruption of molecular planarity and symmetry. *J. Med. Chem.* **2011**, *54*, 1539−1554.

(13) Kang, D.; Feng, D.; Sun, Y.; Fang, Z.; Wei, F.; De Clercq, E.; Pannecouque, C.; Liu, X.; Zhan, P. Structure-based bioisosterism yields HIV-1 NNRTIs with improved drug-resistance profiles and favorable pharmacokinetic properties. *J. Med. Chem.* **2020**, *63*, 4837−4848.

(14) Kang, D.; Ruiz, F. X.; Feng, D.; Pilch, A.; Zhao, T.; Wei, F.; Wang, Z.; Sun, Y.; Fang, Z.; De Clercq, E.; Pannecouque, C.; Arnold, E.; Liu, X.; Zhan, P. Discovery and characterization of fluorine-substituted diarylpyrimidine derivatives as Novel HIV-1 NNRTIs with highly improved resistance profiles and low activity for the hERG ion channel. *J. Med. Chem.* **2020**, *63*, 1298−1312.

(15) Huang, B.; Chen, W.; Zhao, T.; Li, Z.; Jiang, X.; Ginex, T.; Vílchez, D.; Luque, F. J.; Kang, D.; Gao, P.; Zhang, J.; Tian, Y.; Daelemans, D.; De Clercq, E.; Pannecouque, C.; Zhan, P.; Liu, X. Exploiting the tolerant region I of the non-nucleoside reverse transcriptase inhibitor (NNRTI) binding pocket: discovery of potent diarylpyrimidine-typed HIV-1 NNRTIs against wild-type and E138K mutant virus with significantly improved water solubility and favorable safety profiles. *J. Med. Chem.* **2019**, *62*, 2083−2098.

(16) Bauman, J. D.; Das, K.; Ho, W. C.; Baweja, M.; Himmel, D. M.; Clark, A. D., Jr.; Oren, D. A.; Boyer, P. L.; Hughes, S. H.; Shatkin, A. J.; Arnold, E. Crystal engineering of HIV-1 reverse transcriptase for structure-based drug design. *Nucleic Acids Res.* **2008**, *36*, 5083−5092.

(17) Das, K.; Bauman, J. D.; Clark, A. D., Jr.; Frenkel, Y. V.; Lewi, P. J.; Shatkin, A. J.; Hughes, S. H.; Arnold, E. High-resolution structures of HIV-1 reverse transcriptase/TMC278 complexes: strategic flexibility explains potency against resistance mutations. *Proc. Natl. Acad. Sci. U.S.A.* **2008**, *105*, 1466−1471.

(18) Otwinowski, Z.; Minor, W. Processing of X-ray diffraction data collected in oscillation mode. *Methods Enzymol.* **1997**, *276*, 307−326.

(19) Adams, P. D.; Afonine, P. V.; Bunkóczi, G.; Chen, V. B.; Davis, I. W.; Echols, N.; Headd, J. J.; Hung, L.-W.; Kapral, G. J.; Grosse-Kunstleve, R. W.; McCoy, A. J.; Moriarty, N. W.; Oeffner, R.; Read, R. J.; Richardson, D. C.; Richardson, J. S.; Terwilliger, T. C.; Zwart, P. H. PHENIX: a comprehensive python-based system for macromolecular structure solution. *Acta Crystallogr., Sect. D: Biol. Crystallogr.* **2010**, *66*, 213−221.

(20) Emsley, P.; Cowtan, K. Coot: model-building tools for molecular graphics. *Acta Crystallogr., Sect. D: Biol. Crystallogr.* **2004**, *60*, 2126−2132.

(21) Kang, D.; Feng, D.; Ginex, T.; Zou, J.; Wei, F.; Zhao, T.; Huang, B.; Sun, Y.; Desta, S.; De Clercq, E.; Pannecouque, C.; Zhan, P.; Liu, X. Exploring the hydrophobic channel of NNIBP leads to the discovery of novel piperidine-substituted thiophene[3,2-d]pyrimidine derivatives as potent HIV-1 NNRTIs. *Acta Pharm. Sin. B* **2020**, *10*, 878−894.

(22) Kang, D.; Sun, Y.; Murugan, N. A.; Feng, D.; Wei, F.; Li, J.; Jiang, X.; De Clercq, E.; Pannecouque, C.; Zhan, P.; Liu, X. Structure-activity relationship exploration of NNIBP tolerant region I leads to potent HIV-1 NNRTIs. *ACS Infect. Dis.* **2020**, *6*, 2225−2234.

(23) Kuroda, D. G.; Bauman, J. D.; Challa, J. R.; Patel, D.; Troxler, T.; Das, K.; Arnold, E.; Hochstrasser, R. M. Snapshot of the equilibrium dynamics of a drug bound to HIV-1 reverse transcriptase. *Nat. Chem.* **2013**, *5*, 174−181.

(24) Sarafianos, S. G.; Marchand, B.; Das, K.; Himmel, D. M.; Parniak, M. A.; Hughes, S. H.; Arnold, E. Structure and function of HIV-1 reverse transcriptase: molecular mechanisms of polymerization and inhibition. *J. Mol. Biol.* **2009**, *385*, 693−713.

(25) Darby, J. F.; Hopkins, A. P.; Shimizu, S.; Roberts, S. M.; Brannigan, J. A.; Turkenburg, J. P.; Thomas, G. H.; Hubbard, R. E.; Fischer, M. Water networks can determine the affinity of ligand binding to proteins. *J. Am. Chem. Soc.* **2019**, *141*, 15818−15826.

(26) Schiebel, J.; Gaspari, R.; Wulsdorf, T.; Ngo, K.; Sohn, C.; Schrader, T. E.; Cavalli, A.; Ostermann, A.; Heine, A.; Klebe, G. Intriguing role of water in protein-ligand binding studied by neutron crystallography on trypsin complexes. *Nat. Commun.* **2018**, *9*, 3559.

(27) Rudling, A.; Orro, A.; Carlsson, J. Prediction of ordered water molecules in protein binding sites from molecular dynamics

simulations: the impact of ligand binding on hydration networks. *J. Chem. Inf. Model.* **2018**, *58*, 350−361.
(28) Huo, Z.; Zhang, H.; Kang, D.; Zhou, Z.; Wu, G.; Desta, S.; Zuo, X.; Wang, Z.; Jing, L.; Ding, X.; Daelemans, D.; De Clercq, E.; Pannecouque, C.; Zhan, P.; Liu, X. Discovery of novel diarylpyrimidine derivatives as potent HIV-1 NNRTIs targeting the "NNRTI adjacent" binding site. *ACS Med. Chem. Lett.* **2018**, *9*, 334−338.
(29) Kang, D.; Huo, Z.; Wu, G.; Xu, J.; Zhan, P.; Liu, X. Novel fused pyrimidine and isoquinoline derivatives as potent HIV-1 NNRTIs: a patent evaluation of WO2016105532A1, WO2016105534A1 and WO2016105564A1. *Expert Opin. Ther. Pat.* **2017**, *27*, 383−391.

https://doi.org/10.1021/acs.jmedchem.1c00268
J. Med. Chem. 2021, 64, 4239−4256